Experimental and CFD Simulation Study of Binary Solid-Liquid Fluidized Bed

A Project submitted to the

National Institute of Technology, Rourkela

In partial fulfillment of the requirements

Master of Technology

in

Chemical Engineering

By

Ms. Sanjukta Bhoi

Roll no. - 210CH1200

Department of Chemical Engineering

National Institute of Technology,

Rourkela 769008, India

Experimental and CFD Simulation Study of Binary Solid-Liquid Fluidized Bed

A Project submitted to the

National Institute of Technology, Rourkela

In partial fulfillment of the requirements

Master of Technology

in

Chemical Engineering

By

Ms. Sanjukta Bhoi

Roll no. - 210CH1200

Under the Supervision of

Prof. (Dr.) K.C. Biswal

Department of Chemical Engineering

National Institute of Technology,

Rourkela 769008, India

Department of Chemical Engineering
National Institute Of Technology, Rourkela
Odisha -769 008, India

Certificate

This is to certify that the project report entitled **"Experimental and CFD Simulation Study of Binary Solid-Liquid Fluidized Bed"** submitted by Miss Sanjukta Bhoi, Roll No-210CH1200 to National Institute of Technology, Rourkela is for the partial fulfillment of the requirements for the degree of Master of Technology (Chemical Engineering) is an authentic work carried out by her under my supervision and guidance.

Date:

Supervisor

Prof. Dr. K.C. Biswal

Dept. of Chemical Engineering

National Institute of Technology,

Rourkela – 769008

Acknowledgement

I feel immense pleasure and privilege to express my deep sense of gratitude, indebtedness and thankfulness to Prof. Dr. K.C. Biswal who have helped, inspired and encouraged me and also for his valued criticism during the preparation of my M.Tech Thesis work.

I am also indebted to scientist Dr. S.K. Biswal and Mr. Alok Tripathy, Minral Processing Department, CSIR-IMMT, Bhubaneswar for their invaluable guidance, inspiration and encouragement given to me at all stages of my project work.

I am also grateful to Prof R. K. Singh, Head of the Department, Chemical Engineering for providing the necessary facilities for the project.

I am also thankful to all the staff and faculty members of Chemical Engineering Department, National Institute of Technology, Rourkela for their consistent encouragement.

I would like to extend my sincere thanks to my friends and colleagues. Last but not least I am also thankful to Mr. Sambhurisha Mishra for his unconditional assistance and support.

Date:

Miss Sanjukta Bhoi

Roll No- 210ch1200

Contents

		Page no.
Abstract		i
List of Tables		ii
List of Figures		iii
Nomenclatures		vi
CHAPTER 1	INTRODUCTION	
1.0	Introduction	1
1.1	Advantages of Fluidization	2
1.2	Application of Fluidization	2
1.3	Disadvantages of Fluidization	3
1.4	Complexity of Fluidization	3
1.5	Objective of the Work	4
1.6	Outline of the project	5
CHAPTER 2	LITERATURE SURVEY	
2.0	Introduction	6
2.1	Types of Fluidization	6
2.1.1	Particulate Fluidization (Liquid-Solid Fluidization System)	6
2.1.2	Aggregative Fluidization (Gas-Solid Fluidization System)	7
2.2	Bed Expansion	8
2.2.1	Steady State Bed Expansion	8
2.2.2	Unsteady State Behavior of Liquid Suspension	8
2.2.3	Prediction of Total Bed Expansion	8
2.3	Previous Work	9
2.3.1 Experimental Survey		9
2.3.2 Computational Survey		12
CHAPTER-3	EXPERIMENTAL SET-UP AND TECHNIQUES	
3.0	Introduction	19
3.1	Experimental Set-Up	19
3.2	Constituent of Experimental Set-Up	20

3.3	Materials and Methods	22
3.4	Experimental Procedure	23
CHAPTER-4	BED EXPANSION OF BINARY PARTICLE SYSTEM IN FLUIDIZED BED	
4.0	Introduction	24
4.1	Experimental Set-Up and Techniques	24
4.2	Experimental	25
4.3	Results and Discussion	25
4.4	Conclusion	35
CHAPTER-5	CFD SIMULATION OF HYDRODYNAMIC CHARACTERISTIC OF BINARY MIXTURE	
5.1	CFD (Computational Fluid Dynamics)	36
5.2	Advantages of CFD	37
5.3	CFD Modeling of Multiphase Systems	37
5.4	Disadvantages of CFD	38
5.5	Application of Computational Fluid Dynamics (CFD)	38
5.6	Approaches to Multiphase Modeling	38
5.6.1	The Euler-Lagrange Approach	39
5.6.2	The Euler-Euler Approach	39
5.7	Choosing a Multiphase Model	40
5.8	Computational Flow Model	41
5.8.1	Governing Equations	41
5.8.2	Turbulence Modeling	42
5.8.3	Discretization	43
5.8.4	Geometry and Mesh	44
5.8.5	Selection of Models for Simulation	44
5.8.6	Boundary and Initial Conditions	45
5.8.7	Solution Controls	45
5.9	Results and Discussions	47
5.10	Conclusions	58
CHAPTER-6	CONCLUSION AND FUTURE SCOPE OF THE WORK	60
CHAPTER-7	REFERENCE	62

Abstract

Solid liquid fluidization experiments were carried out for binary mixture of iron ore-quartz and chromite-quartz. All the experiments were performed with close size range particles to reduce the size and shape effect of the particles. It has been found that weight ratio of flotsam and jetsam affect the expansion of the fluidized bed. It was also found that particle density affect the bed expansion and other hydrodynamic characteristics. Also a feed for liquid/solid fluidization observed three types of binary system, (a) easily separable (b) difficult to separate (c) non separable. For an unstable binary fluidized bed system corresponding to a pure heavier particle bottom of the bed, lighter particles segregate at the top, and some particles neither segregate nor sink, and they missed place at the middle. Therefore knowing the physical properties of the mineral particles, an appropriate fluidization can be chosen.

The objective of the CFD analysis in this study is to investigate numerically the hydrodynamic behaviour of a liquid- solid fluidized bed. The methodology used in CFD to solve problems relating mass, momentum and heat transfer and the details about problem description and approach used in ANSYS FLEUNT 13.0 to get the solution. Finally results of simulation and comparison with experimental results are shown. CFD predicts the flow characteristics, bed hydrodynamics etc. The simulation is done for a column of 150cm height and 10cm diameter filled with 125μm iron ore, chromite and quartz mixture till a certain height. It is observed that the bed expands considerably with increase in water velocity.

Key Word: Liquid-solid fluidization, segregation, bed expansion, flotsam, jetsam, CFD

List of Tables

Table No.	Title	Page No.
Table-3.1	Properties of Fluid and Solid Phases	22
Table-4.1	Effect of different weight ratio and stagnant bed height of binary mixture of iron ore and quartz on pressure drop	26
Table-4.2	Effect of different weight ratio and stagnant bed height of binary mixture of chromite ore and quartz on pressure drop	27
Table-4.3	Effect of different weight ratio and stagnant height of binary mixture of iron ore and quartz on bed expansion	28
Table-4.4	Effect of different weight ratio and stagnant bed height of binary mixture of chromite and quartz on bed expansion	29
Table-4.5	Wt. % of iron ore and quartz	30
Table-4.6	Wt. % of chromite and quartz	31
Table -4.7	Effect of weight ratio on the jetsam distribution along the expanded bed height for iron ore and quartz mixture	31
Table -4.8	Effect of weight ratio on the jetsam distribution along the expanded bed height for chromite and quartz mixture	32
Table -4.9	Effect of overall voidage along the expanded bed height for iron ore and quartz mixture	34
Table -4.10	Effect of overall voidage along the expanded bed height for chromite and quartz mixture	35
Table-5.1	Model constants used for simulation	44

List of Figures

Fig. No.	Title	Page No.
Fig.3.1	Schematic diagram of experimental setup	20
Fig.3.2	Experimental set-up	21
Fig.4.1	Variation of bed pressure drop with water superficial velocity for different weight ratio and stagnant bed height of iron ore and quartz mixture.	25
Fig.4.2	Variation of bed pressure drop with water superficial velocity for different weight ratio and stagnant bed height of chromite and quartz mixture.	27
Fig.4.3	Variation of bed expansion ratio with water superficial velocity for different weight ratio and stagnant bed height of iron ore and quartz mixture	28
Fig.4.4	Variation of bed expansion ratio with water superficial velocity for different weight ratio and stagnant bed height of chromite and quartz mixture	29
Fig.4.5	Wt % of jetsam Vs bed height for different ratio of iron ore and quartz mixture	32
Fig.4.6	wt. % of jetsam vs. bed height for different ratio of chromite and quartz mixture	33
Fig.4.7	Variation of overall bed voidage with superficial water velocity for different ratio of iron ore and quartz mixture	33
Fig.4.8	Variation of overall bed voidage with superficial water velocity for different ratio of iron ore and quartz mixture	34

Fig.5.1	2D mesh	44
Fig.5.2	Flow diagram for the computational treatment of the equations	45
Fig.5.3	Plot of residuals with the progress of simulation	46
Fig.5.4	Contours of volume fraction of 125µm quartz for Iron ore and Quartz mixture at water velocity of 0.007073 m/s with respect of time for initial bed height 0.1 m	47
Fig.5.5	Contours of volume fraction of 125µm quartz for Chromite and Quartz mixture at water velocity of 0.007073 m/s with respect of time for initial bed height 0.13 m.	48
Fig.5.6	Contours of volume fraction of iron ore, quartz, water at velocity of 0.007073 m/s for initial static bed height of 0.1 m	49
Fig.5.7	Contours of volume fraction of Chromite, quartz, water at velocity of 0.007073 m/s for initial static bed height of 0.16 m	49
Fig.5.8	Velocity vector of Iron ore, Quartz and Water	50
Fig.5.9	Velocity vector of Chromite, Quartz and Water	51
Fig.5.10	XY plot of velocity magnitude of liquid phase	51
Fig.5.11	Contour plot of iron ore and Quartz volume fraction with variation in liquid velocity	52
Fig.5.12	Contour plot of Chromite and Quartz volume fraction with variation in liquid velocity	53
Fig.5.13	XY plot of Iron ore and Quartz volume fraction	53
Fig.5.14	(a) CFD simulation of Bed expansion behaviour at Hs =0.1m (b) Comparison of bed height obtained from simulated and the	54

	experimental values for iron ore and quartz	
Fig.5.15	(a) CFD simulation of bed expansion behaviour at Hs=0.16 m (b) comparison of bed height obtained from simulated and the experimental values for chromite and quartz mixture	54
Fig.5.16	CFD simulation result of expanded bed height vs. superficial liquid velocity at different weight ratio of iron ore and quartz mixture	55
Fig.5.17	Comparison of bed height vs. superficial liquid velocity obtained from experimental and CFD simulation	56
Fig.5.18	mixing and segregation at a velocity 0.000707 m/s and 0.007073 m/s results obtain from CFD simulation	56
Fig.5.19	Variation of bed pressure drop with superficial water velocity for different weight ratio of mixtures results obtain from CFD simulation	57
Fig.5.20	Variation of pressure drop vs. bed height for different weight ratio of 40:60 for different velocity of mixtures results obtain from CFD simulation	57
Fig.5.21	Variation of pressure drop vs. radial distance for different bed height of mixtures results obtain from CFD simulation	58

Nomenclature

U	superficial liquid velocity, m/s
U_t	terminal settling velocity of particle, m/s
ε	beb voidage
x_i	volume fraction on a dry basis in the mixture
n	Rechardson Zaki exponent
u_k	liquid and solid velocity, m/s
C_D	drag coefficient
I	identity matrix
Re_S	Reynolds number based upon the interstitial liquid velocity
μ_s	bulk viscosity of solid, kg/ms
μl	molecular viscosity of fluid, kg/ms
μ_t	turbulent (or eddy) viscosity,
ε_k	volume fraction of liquid and solid phases
λ_k	bulk viscosity of liquid and solid phases
ρ_k	density of fluid and solid, kg/m^3
P	pressure shared by all phases
$F_{i,s}$	inter-phase momentum exchange term
G_k	generation of turbulence kinetic energy due to the mean velocity gradients
G_b	generation of turbulence kinetic energy due to buoyancy

Y_M	contribution of the fluctuating dilatation in compressible turbulence to the overall dissipation rate
$C_{i\varepsilon}$	constants
σ_k	turbulent Prandtl numbers for k
σ_ε	turbulent Prandtl numbers for ε
S_k, S_ε	user-defined source terms

CHAPTER-1

INTRODUCTION

CHAPTER-1

1.0 INTRODUCTION

Fluidization is the operation by which solid particles are behaves like a fluid through suspension in a liquid or gas. One of the most important features of fluidized beds is their ability to mix and segregate. Fluidization is the preferred method of operation due to its many advantages over other configurations, like; good solid mixing leading to uniform temperature throughout the bed, high mass and heat transfer rates, easy solids handling, ability to maintain a uniform temperature, significantly lower pressure drops which reduce pumping costs, lower investments for the same feed and product specifications, yielding large axial dispersion of phases, etc.

On passing fluid (gas or liquid) upward through a bed of fine particles, at a low flow rate fluid merely percolates through the void spaces between stationary particles. This is a fixed bed. With an increase in flow rate, particles move apart and a few are seen to vibrate and move about in restricted regions. This is the expanded bed. At a still higher velocity, the pressure drop through the bed increases. At a certain velocity the pressure drop through the bed reaches the maximum and a point is reached when the particles are all just suspended in the upward flowing gas or liquid. At this moment, the particles at the bottom of the bed begin to fluidize, thereafter the condition of fluidization will extend from the bottom to the top and the pressure drop will decline fairly sharply.

Evidently, fluidization is initiated when the force exerted between a particle and fluidizing medium counterbalances the effective weight of the particle, the vertical component of the compressive force between the adjacent particles disappears, and the pressure drop through any section of the bed about equals the weight of fluid and particles in that section. The bed is considered to be just fluidized and referred to as an incipiently fluidized bed or a bed at minimum fluidization. Under the assumption that friction is negligible between the particles and the bed walls, also it is assumed that the lateral velocity of fluid is relatively small and can be neglected and the vertical velocity of the fluid is uniformly distributed on the cross sectional area.

1.1 ADVANTAGES OF FLUIDIZATION

The chief advantage of fluidization are that the solid is vigorously agitated by when the fluid passing through the bed, and the mixing of the solid certifies that there are practically no temperature gradients in the bed even with quite exothermic or endothermic reactions. The smooth, liquid-like flow of particles allows continuous automatically controlled operations with ease of handling. The rapid mixing of solids leads to nearly isothermal conditions throughout the reactor; hence the operation can be controlled simply and reliably. The circulation of solids between two fluidized beds makes it possible to transport the vast quantities of heat produced or needed in large reactors. Heat and mass transfer rates between gas and particles are high when compared with other modes of contacting. The rate of heat transfer between a fluidized bed and an immersed object is high; hence heat exchangers require relatively small surface areas within fluidized bed reactor. [1-3]

There are other several advantages of fluidized beds such as; ability to maintain a constant temperature, considerably lower pressure drops, catalysts may be added to fluidized beds continuously without affecting the hydrodynamic properties of the fluidized bed reactor (catalyst controlled activity), minimized bed plugging and channelling due to the solids movement, investments for the same feed and product specifications is lower, new improved catalysts can replace older catalysts with minimal effort, high macromixing, yielding large axial dispersion of phases, high reactant conversions for reaction kinetics favouring completely mixed flow patterns.[4]

1.2 APPLICATION OF FLUIDIZATION

In the basis of some advantages of the fluidized bed, fluidization technique is widely used in industry for its different useful applications. Primarily it has been used as a mixing process in the chemical industry, where enhanced reaction, combustion, and heat transfer rates are sought. In the mineral industry, this technique is used for separation of mineral particles having different physical properties. Fluidization has been effective in quite a variety of industries from metallurgical roasting to coal conversion, petroleum refinery, agricultural and food processing, pharmaceutical processes and material processes. [5, 6] Extensive use of fluidization began in the petroleum industry with the development of fluid bed catalytic cracking. Three phase

fluidized bed have been applied successfully to many industrial processes such as in hydrogen-oil process for hydrogenation and hydro-desulfurization of residual oil, the H-coal process for coal liquefaction, and Fischer-Tropsch process.[7] Some more applications are, turbulent contacting absorption for flue gas desulphurization, bio-oxidation process for waste water treatment, physical operation such as drying and other forms of mass transfer, biotechnological processes such as fermentation and aerobic waste water treatment, methanol production and conversion of glucose to ethanol, pharmaceutical and mineral industries, oxidation of naphthalene to phathalic anhydride (catalytic), coking of petroleum residues (non-catalytic).

1.3 DISADVANTAGES OF FLUIDIZATION

However there are also some disadvantages of fluidized bed like, catalyst attrition due to particle motion, entrainment and carryover of particles, relatively larger reactor size compared to fixed beds due to bed expansion, catalyst-fluid contact per unit volume is reduced due to bed expansion, low controllability over product selectivity for complex reactions and loss of driving force due to back mixing of particles in case of transfer operations. The other disadvantages to fluidized bed such as: the difficult-to-describe flow of gas, with its large deviation from plug flow and the bypassing of solids by bubbles, represents an inefficient contacting system. The rapid mixing of solids in the bed leads to non-uniform residence times of solids in the reactor. Friable solids are pulverized and entrained by the gas. For noncatalytic operations at high temperature the agglomeration and sintering of fine particles can necessitate a lowering in temperature of operation, reducing the reaction rate. [3]

1.4 COMPLEXITY OF FLUIDIZATION

With the development of computer technology, computational fluid dynamics (CFD) simulation is becoming more and more useful. The availability of advanced technology like commercial computational fluid dynamics (CFD) software and of faster computer processors has revolutionized scientific research in the field of multiphase flow. CFD has become an indispensable tool, for researchers and engineers alike, in solving many complex problems of academic and industrial interest in areas such as fluidization, combustion, oil flow assurance as well as aerospace science. In the field of fluidization, in particular, the use of CFD has pushed the frontier of fundamental understanding of fluid–solid interactions and has enabled the correct

theoretical prediction of various macroscopic phenomena encountered in fluidized beds and CFD has been applied predominantly to single particle species of uniform species. However, its capability for binary particles in liquid fluidized beds received little attention. Indeed many CFD simulations of monocomponent fluidized systems have been carried out by researchers covering the whole range of Geldart classified powders with great success. CFD is intended to include the key mechanisms of important to predict accurate flow and other characteristics fluidized bed for design, scale-up and optimization. The detailed predictive simulation using simulation made modeling more accurate and faster. [8, 9]

1.5 OBJECTIVE OF THE WORK

EXPERIMENTAL:

- The bed expansion of a binary mixture of particles and to calculate the misplacement of particles in different layer of binary mixture in a fluidized bed.
- It focused on the study bed expansion of a binary mixture of the particles having the different weight ratio of a fixed weight of mixture.

COMPUTATIONAL:

- Theoretical analysis and CFD simulation of a fluidized bed reactor for prediction of its hydrodynamic properties.
- To investigate numerically the hydrodynamic behaviour of a liquid-solid fluidized bed mainly the bed pressure drop, minimum fluidization velocity, and bed expansion or bed voidage. Compare simulated results with the experimentally obtained results

1.6 OUTLINE OF THE REPORT

Chapter 1 includes complete introduction of project work including definition, advantages, disadvantages, application and complexity of fluidization.

Chapter 2 includes the extensive literature survey on this topic namely experimental and theoretical development of the binary solid-liquid fluidization. In the theoretical survey, more emphasis is given on computational fluid dynamics (CFD) analyses of it.

Chapter 3 includes experimental set-up and techniques. In this chapter describe the details information about the experimental set-up, methods and procedure. In methods gives the details information of materials.

Chapter 4 deals with bed expansion of binary particle system in fluidized bed. This chapter includes the variation of pressure drop, velocity, different weight ratio of flotsam and jetsam. All the hydrodynamics characteristics give basic information of the variation of bed expansion experimentally in solid-liquid system.

Chapter 5 represents CFD simulation of hydrodynamic characteristic of binary solid-liquid system. The model equation includes the equation of continuity and momentum equation equations. Also gives the details information about the geometry and solution control. CFD simulation results are comparing with the experimental results and it is also verify the hydrodynamic properties.

Chapter 6 represents the overall conclusion and future scope of the project.

CHAPTER-2

LITERATURE SURVEY

CHAPTER-2

LITERATURE SURVEY

2.0 INTRODUCTION

An expanded or fluidized bed is one in which the particles are suspended in a fluid flow but don't substantially move with the bulk flow of that fluid .The classical chemical engineering definition of an expanded bed is one increase in volume up to 50% or 100% over that of bed when static, i.e., with no fluid flow. Now the availability of advanced commercial computational fluid dynamics (CFD) software and of faster computer processors the research has developed for field of multiphase flow. CFD has become an essential tool, for researchers and engineers alike, in solving many difficult problems of educational and industrialized interest in areas such as fluidization, combustion, oil flow affirmation as well as aerospace science. In the field of fluidization, in particular, the use of CFD has pushed the border of fundamental understanding of fluid–solid interactions and has enabled the correct theoretical estimation of various macroscopic phenomena encountered in fluidized beds.

2.1 TYPES OF FLUIDIZATION

On increasing the fluid velocity, up to the point of fluidization flow pattern are usually well described by Darcy's law. However, after the fluidization point two very distinct types of fluid flow are observed:

2.1.1. PARTICULATE FLUIDIZATION (LIQUID-SOLID FLUIDIZATION SYSTEM)

When fluidizing solid with water, the particles move further apart and their motion becomes more vigorous as the velocity is increased, but at a given velocity the bed density is same in all sections of the fluidized bed. This is called particulate fluidization and is characterized by a large but uniform expansion of the bed at high velocities. Here liquid is behaves as the continuous phase.

In this system, solid particles are brought in contact with the liquid and many particles flow in nearly close and the motion of each particle is influenced by the presence of other particle. Thus, simple investigation of the fluid-particle interaction of a single particle is no longer effective but

can be adopted to model the multiple particle system. In that condition, voidage (ε), or volume fraction occupied by fluid, comes into consideration. Richardson and Zaki (1954) proposed an equation and considering the voidage in the system they related the superficial water velocity with the terminal velocity of the particle. They suggested the following equation for fluidized bed:

$$\frac{U}{Ut} = \varepsilon^n \qquad (1)$$

Where exponent n is a function of particle Reynolds number.

For Ret < 0.2 n = 4.65

0.2 < Ret < 1 n = 4.45 Ret−0.03

1 < Ret < 500 n = 4.45 Ret−0.1

Ret > 500 n = 2.39

Richardson and Zaki shows that voidage plays an important role in liquid/solid fluidization from the above empirical expression. It controls drag in turn controls terminal velocity of the particle.

The particles tend to segregate when particles with different size or density, coarse or heavier particles sink to the bottom and fine or lighter particles entrain from the top of the bed. The particles that sink to the bottom are known as the jetsam phase and the floating particles are termed as flotsam phase. [10]

2.1.2. AGGREGATIVE FLUIDIZATION (GAS-SOLID FLUIDIZATION SYSTEM)

Beds of solids fluidized with air usually it is known as aggregative or bubbling fluidization. In this case gas is used as the continuous phase. At superficial velocities larger than minimum fluidization velocity (V_{mf}) most of the gas passes through the bed as a bubbles or voids which are almost free of solids, and only a small fraction of the gas flows in the channels between the particles.

2.2 BED EXPANSION

An expanded fluidized bed or expanded bed height is one in which the particles are suspended in a fluid flow but don't substantially move with the bulk flow of that fluid .The classical chemical engineering definition of an expanded bed is one increase in volume up to 50% or 100% over that of bed when static, i.e., with no fluid flow. Beds consisting of uniform particles of single size smooth expansion occur as increased the liquid velocity from the minimum fluidizing velocity to the free falling velocity of the particles.

2.2.1. STEADY STATE BED EXPANSION

In this case liquid beds expand in a homogeneous manner. On the other hand, a sharp and flat, interface between the top of the suspension and the freeboard is generally preserved and particles have a considerable size spread and/or very low concentrations are involved. Due to the large number of publish literature available the production of experimental data on liquid fluidized bed expansion is not difficult and also it is not that much important to help in the study of solid-liquid fluid dynamic interaction. Moreover, bed expansion data are generally reported and bed voidage as function of the superficial velocity it is compare with the experimental results. [11]

2.2.2. UNSTEADY STATE BEHAVIOR OF LIQUID SUSPENSION

In this case the physical properties like concentration and velocity is assumed to be no longer constant, a more complete description of the phenomena can be developed from the basic conservation equations for flow: continuity and momentum equations for the solid and fluid phases. [11]

2.2.3. PREDICTION OF TOTAL BED EXPANSION

Sometimes it is of practical interest to know the overall expansion characteristics of a fluidized bed of mixed particles. If the particle characteristics fairly close, one can imagine solid phase behave as monocomponent by utilizing some average of particle size and density. On the other hand, when the solids particles fluidized in separate layers, the overall bed height obtained though the equation.

$$\frac{1}{1-\varepsilon} = \sum \frac{xi}{1-\varepsilon i} \qquad (2.1)$$

Where εi is the voidage of solid i is fluidized alone and xi is its volume fraction on dry basis in the mixture. The first approach relates the solids are completely mixed, the second solids completely segregated. In intermediate situations, neither approach is conceptually exact as the degree of mixing is not taken into account; however the difference between calculated (eq.2.1) and experimental data is generally very low. [12]

2.3 PREVIOUS WORK

2.3.1 EXPERIMENTAL SURVEY

When a mixture of binary particles having sufficiently different physical properties is particulately fluidized under the mechanism of separation of mineral particles in presence of some operating conditions the mixture separates and displays a behavior called layer inversion. Experimental observations are observed to support the theory. There are two case study (1) a binary particles of any type having variation of both size and density or only size variant or only density variant to separate or mix and invert; and (2) mixing or separation occurs of size ratio and density ratio of the particles for a given fluidizing medium. Therefore, appropriate fluidization conditions can be preferred to know the physical properties of mineral particles in order to separate them. [13]

In liquid-fluidized bed binary (and ternary) mixtures of Teflon spheres, discs and rods were taken. All particles had the same volume, while sphericity is nearly same in case of discs and rods. When binary mixtures of different size or density are fluidized, segregation can occur by shape, with similar segregated and mixed zones. [14]

Fluidization of a two particles species under the steady state condition, having different diameters and densities were taken. Steady state mixing solutions of the volume-averaged equations of motion for the fluid and particles are required. To adjacent the continuum equations of motion using a debarred volume assumption an expression for the fluid– particle interactive force (in the mixture) is proposed. Solutions to the equations are found for a fluidized bed of

different particle in water. Comparisons with experimental data recommend that the hydrodynamic mechanism of fluid–particle interaction is not fully taken with an excluded volume assumption. Thus, experimental data can be used to derive expressing of the complex hydrodynamic behavior within the characteristics of the model. [15]

To study the fluidization behavior and hydrodynamic characteristics of liquid-solid fluidization of binary mixtures, the size ratios ranging from 1.2 to 5.13 using sand of different sizes in tapered beds of apex angles 50, 100 and 150. Water is taken as the fluidizing medium. Three types of fluidization behavior have been observed i.e.; (1) mono component behavior, (2) partially segregated behavior and (3) completely segregated behavior. [16]

An experimental work is carried out to clarify the density differences between components play an important role in the segregating fluidization process of two-solid beds. The overall behavior of such systems is considered "minimum fluidization velocity" of the binary mixture with the "velocity interval of fluidization" of the bed, which is in the range of "initial" and "final" fluidization velocity. [17]

Solid–liquid fluidized beds containing binary mixture (Reynolds number range from 0.02 to 2250) and terminal settling velocity (ratios from 1.1 to 2.1) was taken by Epstein et al. (1981). For prediction the overall solid hold-up of the bed they have been used the series type of model, where the mixed bed behaves as if it were simply the sum of the N single species beds. They show the applicability of series model to binary particle mixtures having different sizes and density by explaining large number of experiments. [18]

The fluidization technique has been taken for particulate material processing operations to controls the separation efficiency in case of ratio of size and density of the particulate components. During fluidization the principal significance is the fluid velocity when required an improvement in separation efficiency. To analyzing simpler particulate systems first experimentally established and later to study a wider range of particulate systems a simulation scheme was adopted. Discrete element method (DEM) incorporates both the solid and hydrodynamic components of the interactive forces, worked as an important tool for understanding the separation behavior of binary particulate systems in fluidized beds. [19]

A binary liquid fluidized bed system not at a stable equilibrium condition hence it is modeled in the literature as making a mixed part corresponding to stable mixture at the bottom of the bed and a pure layer of excess components always floating on the mixed part. Binary particles of any type to mix or segregate and mixing or segregation can occur in terms of size ratio and density ratio of the particles for a given fluidizing medium on the basis of this model. Therefore, mixing or segregation can occurs in terms of size ratio and density ratio of the particles for knowing the properties of given particles. Hence multicomponent fluidized bed is advanced for the model and model is corroborated against experimental results. [20]

The flow characteristics of inverse fluidization developing low density spherical particles for both the liquid-solid and gas-liquid-solid systems in experimental investigation. In the liquid-solid system experimental data for the bed expansion correlated in case of empirically as well as semi-empirically. The gas and liquid flows behaves countercurrent in the gas-liquid-solid system and two modes of fluidization obtained. Fluidization occurs with the liquid as a continuous phase or the gas as a continuous phase; and finally characterizes the inverse gas-liquid-solid fluidized bed and the turbulent contacting bed. The inverse gas-liquid-solid fluidization proposed for the correlations of the bed expansion and gas hold-up are. [21]

Component densities and mixture composition is clarified by several series of experiments The dependence of the characteristic velocities on parameters such as by the fluidized bed characterized by minimum fluidization velocity of the binary mixture with the “velocity interval” of fluidization of the bed, which is limited by its “initial and final fluidization velocity”. The experimental results analyzed in the fundamental theory, so as to justify their calculation. [22]

Due to the variation of superficial velocity in the axial direction of the beds, the hydrodynamic characteristics of fluidization in conical or tapered beds differ from those in cylindrical beds. Because the detailed visualization of fluid and particle clearly observed and measurements of the pressure drops is simple in different flow regimes. The tapering angle of the beds affects the beds behavior. Other hydrodynamic characteristics included the minimum velocity of partial fluidization, maximum pressure drop, maximum velocity of partial defluidization, minimum velocity of full fluidization and maximum velocity of full defluidization determined experimentally. The hydrodynamic characteristics of liquid-solid tapered fluidized beds quantify

the proposed model. The results obtained from the models compare with experimental data. Naturally, the models applicable to liquid-solid cylindrical fluidized beds with tapering angle of zero corresponding to the tapered beds. [23]

Using air as fluidizing medium segregation was observed experimentally. The binary mixture of solid particles of same size used as a feed, but having different density. The variables include superficial gas velocity, solids feed rate and feed composition. A physical equilibrium is observed between the evolved flotsam and the residual jetsam at steady state when the granular solids behave like a fluid state. The distribution of the flotsam and jetsam shows the segregation in the fluidized bed and, which clarify the analogy with the distillation of the binary mixture of liquid. Equilibrium distribution of the flotsam and jetsam studied in the effect of the solids feed rate and feed composition. [24]

For the calculation of the pressure gradient drag force, and friction factor for sedimenting suspensions and fluidized beds of uniform spherical particles in liquids a new method is developed. A comparison was made with previous methods of correlation. The relationship between the various drag coefficients for particles in concentrated suspensions is explained. Determining the value of the drag coefficient to established role of the particle-to-vessel diameter ratio. [25]

2.3.2 COMPUTATIONAL SURVEY

Computational Fluid Dynamics (CFD) modeling has been used to simulate a liquid fluidized bed of lead shot in slugging mode. The commercial codes CFX4.4 are used to perform the simulations. The kinetic model for granular flow, already available in CFX, has been used for this study and 2D time-dependent simulations have been carried out at different water velocities. Simulated aspects of fluidization such as voidage profiles, slug formation, pressure drop and pressure fluctuations have been analysed and was found that the fluid-bed pressure drop was greater than the theoretical values at all velocities, which is in agreement with experimental observations reported for fully slugging fluidized beds. To investigate the development of the flow pattern and the structure of the fluid-bed with increasing fluidizing velocity power spectral density analysis of the pressure signal was used. [26]

CFD simulations were performed for the prediction of segregation and/or intermixing of binary particle systems having the ratio of different terminal settling velocity. The Reynolds number has also been varied for the different range. It has been observed that the present CFD model that all the qualitative and quantitative observations and their predictions were in good agreement with the experimental results and their CFD model also predicts successfully the layer inversion phenomena which occur in the binary particle mixtures of different size as well as density. [27]

CFD modeling of fluidized beds can be classified in to Eulerian–Lagrangian and Eulerian–Eulerian approaches. Eulerian–Lagrangian models describes the fluid flow using the continuum equations, and the particulate phase flow is described by tracking the motion of individual particles, but due to the computational limitations, the Eulerian–Lagrangian models are normally limited to a relatively small number of particles. Therefore, the other approach, Eulerian–Eulerian continuum modeling, in which fluid and solid phases are treated as interpenetrating continuum phases, is the most commonly used approach in the fluidized bed simulations (Ding and Gidaspow, 1990). [28]

The Eulerian–Eulerian fluid dynamic model for monodisperse suspensions of solid particles fluidized by Newtonian incompressible fluids in a homogeneous fluidized bed. The closure relationships for the fluid–particle interaction force distinguish the proposed equations of motion. The buoyancy, local fluid acceleration, drag and elastic forces comprises the force. To test the drag force closure, the steady state expansion profiles of liquid fluidized systems were evaluated computationally, and were compared with those obtained using the closures of Wen and Yu and Ergun. Analytical and computational results (obtained by linear stability analysis and integration of the equations of motion, respectively) were compared with experimental findings. [29]

It is a well known fact that understanding hydrodynamics of liquid-solid fluidized beds is crucial in proper scale-up and design of these reactors. And in such a condition Computational fluid dynamics (CFD) models have played a vital role. A two-dimensional CFD model, using an Eulerian Eulerian two-fluid model incorporating the kinetic theory of granular flow, has been used to describe the liquid-solid two-phase flow in a liquid-solid fluidized bed. The predicted pressure gradient data and concentrations were found to agree with experimental data. Furthermore, the model was used to investigate the influences of the superficial liquid velocity and the solid particle size on the distribution of solids concentration. The simulation results

showed that the solids concentration had a relatively uniform distribution and high bed expansion with the increase of liquid velocity and decrease of particles sizes and Solids mean axial velocities decreased with the decrease in superficial liquid velocity. [30]

Long Fan at el. proposed unsteady laminar flow simulated by a modified two-dimensional Eulerian-Eulerian model in Fluent 6.3 and then predictions were compared with experimental results for binary particles in the same narrow size range, but with different densities fluidized by water. The voidages and heights of two layers which form, each dominated by one particle species, were found to be sensitive to small changes in particle properties (diameter, density, sphericity), as well as temperature (because of its effect on the water viscosity). As a result, agreement between simulations and experimental results depends on several incompletely characterized factors. [31]

The effects of mesh size, time step and convergence criteria were investigated. Simulations and comparisons were carried out using two different liquid distributors (uniform and non-uniform), but a better representation of the geometry of the distributor plate hardly influenced the results. Qualitatively, the simulations showed trends similar to experimental trends reported by various aresearchers. The predictions are also compared with new experimental results for different materials at a wide variety of superficial liquid velocities and two different temperatures significantly affecting the liquid viscosity. The CFD model predictions are within 5% of the steady-state experimental data and showed the correct trend with variation in viscosity [32].

A preliminary CFD study was done to observe the effect of the particle- particle interphase momentum transfer on the mixing and bubble dynamics of a binary gas solid fluidized consisting of particles which only differed in size. A new fluid dynamic model, implemented within a commercial CFD code, CFX4.4, was used to model the binary mixture. The solids pressure for each of the particulate phases was not taken into consideration in this model, however solid phase compaction for the each of the particulate phases was controlled via a numerical scheme supporting experimental validation of the computational results was also presented herein. Results from the CFD simulations in agreement with the experimental results, initially showed an increase in bubble diameter at increasing bed height however the trend discontinued higher up in the bed, with the simulation in which particle-particle drag force was neglected giving the poorest agreement. [33]

A model was presented for the prediction of the fluid dynamic behaviour of binary suspensions of solid particles fluidized by Newtonian fluids. The equations of motion for the fluid and solid phases were derived by extending the averaged two-fluid equations of change for identical spheres in Newtonian fluids developed by Anderson and Jackson and Jackson. A new closure relationship for the fluid–particle interaction force was employed and to control the solid compaction in each particle phase a new numerical algorithm was developed. To validate the predictions of the fluidization behavior obtained by the proposed model it was compared with the experimental results in terms of solid mixing and segregation, bed expansion and bubble dynamics. Two-dimensional CFD simulations were performed in a bed of rectangular geometry using ballotini with particle sizes of 200 and 350 μm. [34]

Though the published work on CFD modeling of fluidized beds is mostly on the gas-solid fluidized beds, a few CFD studies are available on the solid–liquid fluidized beds. This CFD simulations have shown the gradual development of the slugging regime with the increase of the superficial liquid velocity. Cornelissen et al. (2007) have simulated the solid–liquid fluidized bed using glass particles with different superficial liquid velocities using multi fluid Eulerian model. They also used Wen and Yu (1966) and Gidaspow (1994) drag laws for the momentum exchange between the two phases. They investigated the effects of mesh size, time step and convergence criteria on the bed expansion. The drag laws used in the published literature have been summarized below [35]:

(1) Wen and Yu (1966) drag law (liquid-solid):

$$K_{ls} = 3C_D \frac{\varepsilon_s \rho_s v_s^2}{d_p} \varepsilon_l^{-2.65} \quad (2.2)$$

Where $C_D = \frac{24}{\varepsilon_l Re_s} [1 + 0.15(\varepsilon_l Re_s)^{0.687}]$

(2) Syamlal and O'Brien (1989) drag law:

$$K_{ls} = 3C_D \frac{\varepsilon_s \rho_s v_s}{d_p \beta^3} Re_s \quad (2.3)$$

Where $C_D = (0.63 + \frac{4.8}{\sqrt{Re_s/\beta}})^2$

$\beta = \frac{1}{2}(A - 0.06Res + \sqrt{(0.06Re_s)^2 + 0.12Re_s(2B - A) + A^2})$

For $\varepsilon_l \leq 0.85$ $\quad A = \varepsilon_l^{4.14} \quad B = \varepsilon_l^{1.28}$

For $\varepsilon_l > 0.85$ $\quad A = \varepsilon_l^{4.14} \quad B = \varepsilon_l^{2.64}$

(3) Gidaspow (1994) drags law (high dense liquid-solid):

$K_{ls} = 3C_D \frac{\varepsilon_s \varepsilon_l \rho_l V_s^2}{d_p} \varepsilon_l^{-2.65}$ for $\varepsilon_l > 0.8$ (2.4)

$K_{ls} = 150 \frac{\varepsilon_s^2 \mu_l V_S}{\varepsilon_l d_p^2} \varepsilon_l^{-2.65} + 1.75 \frac{\varepsilon_s \rho_l V_s^2}{d_p}$ for $\varepsilon_l \leq 0.8$ (2.5)

Where $C_D = \frac{24}{\varepsilon_l Re_s}[1 + 0.15(\varepsilon_l Re_s)^{0.687}]$

$Re_s = \frac{d_p V_s \rho_l}{\mu_l}$

It may be emphasized that all the above laws are empirical and based on the experimental studies of heterogeneous gas-solid beds where, nonuniformity in the voidage prevails. Therefore, in the present work the drag coefficient(C_D) has been modeled by using the following equations proposed by Joshi (1983) and Pandit and Joshi(1998) which have been derived using energy balance approach [36].

For $Re_\infty < 0.2$ $\quad C_D = \frac{6}{Re_\infty}(\frac{3.6\varepsilon_s}{\varepsilon_l^2} + \varepsilon_l^2)$ (2.6)

For $0.2 < Re_s < 500$ $\quad C_D = \frac{6}{Re_\infty}(\frac{3.6\varepsilon_s}{\varepsilon_l^2} + \varepsilon_l^2) + (C_{DS} + (\frac{2k}{3V_S^2}))$ (2.7)

For $Re_\infty > 500$ $\quad C_D = C_{DS} + (\frac{2k}{3V_S^2})$ (2.8)

These drag equations are based on the total surface area of the particle. For the case of the creeping flow (Re_∞ <0.2) these governing equations are discretized by control volume formulation.

The results obtained from a 'discrete particle method' (DPM) were qualitatively compared to the results obtained from a multi-fluid computational fluid dynamic (CFD) model. The implemented collision model is based on the conservation laws for linear and angular momentum and requires, apart from geometrical factors, two empirical parameters: a restitution coefficient and a friction coefficient. The fluid dynamic model of the gas is based on the volume-averaged Navier–Stokes equations. In the multi-fluid CFD model, also referred as Eulerian–Eulerian (EE), the gas and the solid phases were considered to be continuous and fully inter-penetrating. Both phases were described in terms of separate sets of conservation equations with appropriate interaction terms representing the coupling between the phases. [37]

It is a well known fact that either a well-mixed bed or a segregated bed can be a result of fluidization of dissimilar materials. In a fluidized bed, particle mixing and segregation phenomena are dominated by bubble activity. Depending on operating conditions, lighter or smaller particles (flotsam) tend to rise from the bed, and larger, heavier particles (jetsam) tend to sink to the bottom of the bed. A series of unsteady, three-fluid CFD simulations were performed using FLUENT 6.0. The solids consisted of two dissimilar materials, coke and rutile, with different diameters and densities. Simulation parameters (solution technique, grid, maximum packing fraction, drag law) and operating conditions (gas velocity, bed makeup, nozzle location) were each investigated for the relative effects on bubbling and hence on particle mixing and segregation. [38]

A low Reynolds number k-ε CFD model was used for the description of flow pattern near the wall. An excellent agreement was observed between the predicted and experimental hold-up and velocity profiles over a wide range of superficial gas velocity (VG), column diameter (D), column height (HD) and the nature of gas-liquid system (bubble diameter and their rise velocity). The CFD model was extended for the prediction of pressure drop for two-phase gas-liquid flows in bubble columns. This paper also presented a between the predicted and the experimental data over a wide range of superficial gas and liquid velocities and for three gas-liquid systems. [39]

A computational fluid dynamics model was used to examine the structure of three-phase (air-water-glass beads) flows through a vertical column. To modify the drag between the liquid and the gas phase the study proposed new correlations to account for the effect of solid particles on bubble motion. The study was to propose new correlations for drag between the solid particles and liquid phase to incorporate the effect of the bubbles. Solid-solid interactions were also accounted for in the model by a modification to the drag force acting on the solid phase. A k−ε turbulence model was used for simulating the effect of turbulence on the flow field. Predictions were compared with experimental data for the axial variation of the solids concentration for model validation. [40]

The two-dimensional Eulerian fluid dynamic method, the dispersed particle method (DPM) and the volume-of-fluid (VOF) method was used to account for the flow of liquid, solid and gas phases respectively. A continuum surface force (CSF) model, a surface tension force model and Newton's third law was applied to account for the interphase couplings of gas–liquid, particle–bubble and particle–liquid interactions respectively. A close distance interaction (CDI) model included in the particle–particle collision analysis, which considerd the liquid interstitial effects between colliding particles. Single bubble rising velocity in a liquid–solid fluidized bed and the bubble wake structure and bubble rise velocity in liquid and liquid–solid medium were investigated.[41]

CHAPTER-3

EXPERIMENTAL SET-UP AND TECHNIQUES

CHAPTER-3

EXPERIMENTAL SET-UP AND TECHNIQUES

3.0 INTRODUCTION

Fluidization system has been widely applied in the chemical engineering on different application. It has good potential to apply in mineral processing. In gravity separation process this techniques has been incorporated in jigging, hydrodryer, all flux and also enhance gravity separator. The separation efficiency between different particles depends on the particles dynamics based on their characteristics. To improve the separation efficiency details characteristics on fluidization studies are needed. In this chapter bed expansion on binary particle system was taken.

3.1 EXPERIMENTAL SET-UP

The experimental set-up for fluidization tests consists of a glass cylindrical column of 150 cm height and 10 cm diameter. Fig.3.1 shows the schematic representation of experimental set-up and Fig.3.2 represents the actual set-up. A homogenization chamber fitted at the bottom of the fluidization column of the bed was filled with glass beads to keep the fluid flow uniform across the cross section. From the bottom of the fluidization column water was pumped through a rotameter. Rotameter is fixed to a manual valve and to control the flow rate of water into the fluidization column a bypass line was used. The experimental set-up also has provision to measure the flow rate, the bed height, and the pressure drop across the bed during fluidization. The bed heights were read visually with the help of a ruler placed along the length of the column. Two pressure taps, one at the entrance and the other at the exit section of the bed were provided to record the pressure drops. The pressure drop across the bed was measured using a manometer which was one meter long. Mercury (density=13.534 g/ cm^3) was used as the manometric fluid. Liquid (water, ρ=1 g/cm^3 and μ=1cP) used as the fluidizing medium was passed through a receiver. Two rotameters, one for the lower range (0-50 lit/hr.) and the other for the higher range (50-500 lit/hr.) were used to measure the liquid flow rates. Prior to the start of the experiment, first measure the density, volume fraction, and voidage of both constituent particle types of the binary system. The results were then compared and analyzed on the basis of superficial fluid velocity of water, bulk density of the slurry, and dynamic voidage of the column.

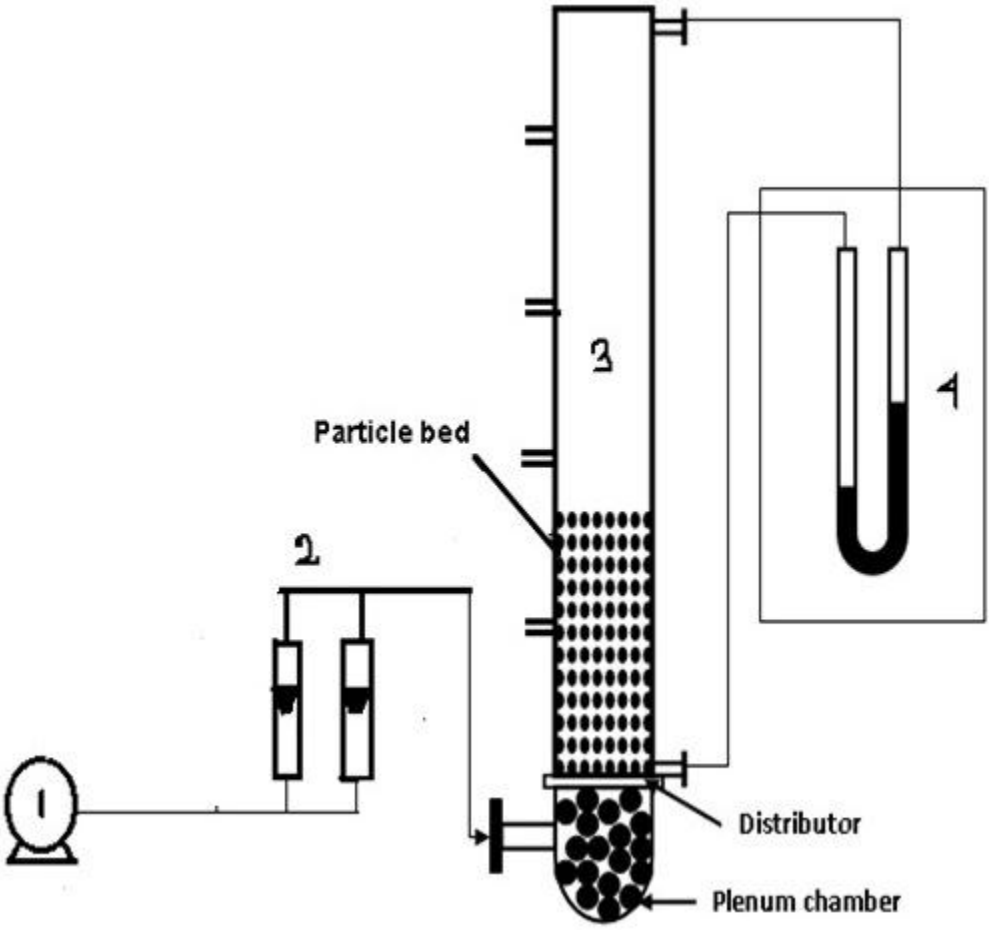

1. Centrifugal pump, 2. Rotameter, 3. Fluidizing column, 4. Manometer

Fig.3.1 Schematic diagram of experimental setup

3.2 CONSTITUENT OF EXPERIMENTAL SET-UP

Centrifugal pump (50 Hz, 1.1 kW, 2900 rpm) is used to move liquids through piping. The fluid enters the pump flowing radially outward into a diffuser or volute chamber (casing), from where it exits into the downstream piping. Centrifugal pump connecting to the water rotameter. Rotameter is used for the measurement of flow rate of water. Two rotameters, one for the lower range (0-50 lt/hr) and the other for the higher range (50-500 lt/hr) were used to measure the flow rates.

During the experiment there is a chance for the generation of fines which may be entrained from the bed. To prevent particle entrainment a 100 micron mesh screen at the bottom served as the support as well as the distributor. The distributor is an integral part of calming section where it is followed by a cylindrical section. The inside hollow space of the distributor which is known as plenum chamber filled with glass beads of 1.5 cm outer diameter, for uniform flow of liquid in the distributor. Plenum is located exactly in axial direction before inlet. The main purpose of the plenum chamber is to provide a relatively turbulent-free region at the inlet to the inlet guide vane. So it will avoid radial vibration. The fluidizer consists of glass column with one end fixed to flange. The column is 150 cm height and having 10cm diameter. It has number of opening for withdrawing materials. Two pressure tapings are provided for noting the bed pressure drop. Manometer is arranged in the fluidized system for measuring the pressure drop. Mercury (density=13.6 g/cm^3) is used as manometric liquid.

Fig.3.2 Experimental set-up

3.3 MATERIALS AND METHODS

The experiments were carried out in cylindrical glass column. The height of the cylindrical column is 150 cm and dimeter of the column is 10 cm. Three type of materials such as iron ore (density of 5100 kg/m^3), chromite (density of 4100 kg/m^3) and quartz (density of 2610 kg/m^3) were used for the investigation. The mixture i.e. iron ore and quartz or chromite and quartz was taken in to different ratios like 20:80, 30:70, 40:60, 50:50, or vice versa. The diameter of the particles was determined by sieving analysis and the average diameter of particles was 125 μm. The density of the particles was obtained by dividing the weight of the particles by the displaced water volume when the particles were placed into a cylindrical column filled with water. The material properties of fluid phase and distribution material in plenum chamber are given in Table 3.1-table 3.3

Table-3.1

Properties of Fluid and Solid Phases

Material properties fluid phase			
Fluid	Viscosity (kg/m.s)		Fluid density(kg/m3)
Water	0.001		1000
Material properties of solid phase			
Mixture	Particle Size (μm)	Average particle dia. (μm)	Density(kg/m3)
Iron ore	-150+100	125	5100
Chromite	-150+100	125	4100
Quartz	-150+100	125	2610
Distributor material in plenum chamber			
Bed Material	Bed height (m)		Diameter of Glass sphere (cm)
Glass sphere	1.5		1.5
Fluid Velocity	0.0177 cm/s to 0.7073cm/s		

3.4 EXPERIMENTAL PROCEDURE

A weighed amount of material was charged to the bed. The initial stagnant bed height was recorded. Then the flow rate of the liquid was increased incrementally allowing sufficient time to reach a steady state for each increment of the flow rate. The rotameters and manometer readings were noted for each increment in flow rate and the pressure drop and superficial velocity calculated. Liquid flow rate was gradually increased and the corresponding bed pressure drops were measured. When the minimum fluidization was attained, the expanded static bed height was also measured. As the bed fluctuates between two limits of liquid-solid fluidization, heights of the upper and the lower surfaces of the fluctuating bed were measured for each fluid velocity higher than the minimum fluidization velocity. After fluidizing the bed with a particular fluid velocity, it was brought to static condition by closing the liquid supply. The bed was then divided into different layers each of 25 cm height. Each of the layers was drawn applying suction. Finally at a constant flow rate, the fluidized materials were collected in different layers and the distance between each layer is 25cm. Then the collected sample was dried and separated in to a perm roll magnetic separator. After the separation, the separated individual materials was weight and calculate the percentage of weight of individual materials collected in different layers for calculating amount of misplaced materials. In this case also found out the amount of mixing and segregate materials.

CHAPTER-4

BED EXPANSION OF BINARY PARTICLE SYSTEM IN FLUIDIZED BED

CHAPTER-4

BED EXPANSION OF BINARY PARTICLE SYSTEM IN FLUIDIZED BED

4.0 INTRODUCTION

An expanded or fluidized bed is one in which the particles are suspended in a fluid flow but don't substantially move with the bulk flow of that fluid .The classical chemical engineering definition of an expanded bed is one increase in volume up to 50% or 100% over that of bed when static, i.e., with no fluid flow. Bed expansion mainly depends on hydrodynamics characteristics like pressure drop, superficial water velocity, bed expansion ratio, voidage etc. Here this chapter shows the relationship between all the hydrodynamics characteristics and explain its importance.

4.1 EXPERIMENTAL SET-UP AND TECHNIQUES

The experimental set-up for fluidization tests consists of a glass cylindrical column of 150 cm height and 10 cm diameter. Fig.3.1 shows the schematic representation of experimental set-up and Fig.3.2 represents the actual set-up. A weighed amount of material was charged to the bed. The initial stagnant bed height was recorded. Then the velocity of the liquid was increased incrementally allowing sufficient time to reach a steady state for each increment of the flow rate. When the minimum fluidization was attained, the expanded static bed height was also measured. As the bed fluctuates between two limits of liquid-solid fluidization, heights of the upper and the lower surfaces of the fluctuating bed were measured for each fluid velocity higher than the minimum fluidization velocity. After fluidizing the bed with a particular fluid mass velocity, it was brought to static condition by closing the liquid supply. Each of the layers was drawn applying suction. Finally at a constant flow rate, the fluidized materials were collected in different layers and the distance between each layer is 25cm. Then the collected sample was dried and separated in to a perm roll magnetic separator. After the separation, the separated individual materials was weight and calculate the percentage of weight of individual materials collected in different layers for calculating amount of misplaced materials. In this case also found out the amount of mixing and segregate materials.

4.2 EXPERIMENTAL

The present study has been conducted to examine the hydrodynamic behavior viz. the pressure drop, minimum liquid fluidization velocity, bed expansion and mixing-segregation in liquid-solid fluidized bed (as shown in Fig. 3.1) using liquid as the continuous phase. Three type of materials such as iron ore (density of 5100 kg/m^3), chromite (density of 4100 kg/m^3) and quartz (density of 2610 kg/m^3) were used for the investigation. The mixture i.e. iron ore and quartz or chromite and quartz was taken in to different ratios like 20:80, 30:70, 40:60, 50:50, or vice versa. The diameter of the particles was determined by sieving analysis and the average diameter of particles was 125 μm. The density of the particles was obtained by dividing the weight of the particles by the displaced water volume when the particles were placed into a cylindrical column filled with water. The material properties of fluid phase and distribution material in plenum chamber are given in Table 3.1.

4.3 RESULTS AND DISCUSSION

4.3.1 SUPERFICIAL VELOCITY AND PRESSURE DROP

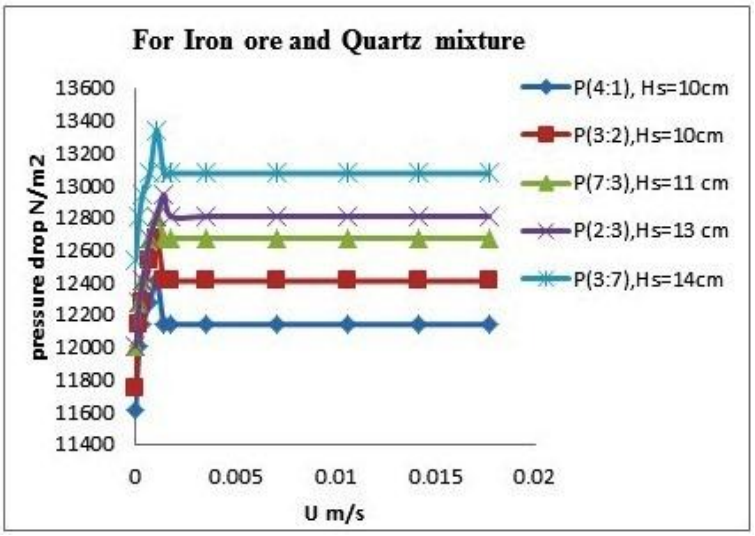

Fig.4.1 Variation of bed pressure drop with superficial water velocity for different weight ratio and stagnant bed height of iron ore and quartz mixture

The Fluidization experiments were carried out using binary mixture of different ratio of iron ore and quartz system and chromite and quartz system at different superficial velocities. Fig.4.1 and Fig.4.2 shows pressure drop as a function of superficial velocity at different static bed height at a same weight. Pressure drop occurs across the bed due to frictional resistance at particle surface and sudden expansion and contraction of flow through interstities among the particles. The pressure drop curves flows the typical nature of a fluidizing system i.e. initially there is increase in the pressure drop with the increase of superficial velocity and once the superficial velocity exceeds the minimum fluidization velocity pressure drop become constant.

Table-4.1

Effect of different weight ratio and stagnant bed height of binary mixture of iron ore and quartz on pressure drop

Flow rate	Superficial velocity	Pressure drop across the bed N/m^2 (Iron ore : Quartz)				
Q lit/hr.	U cm/s	P(4:1), Hs=10cm	P(3:2), Hs=10cm	P(7:3), Hs=11 cm	P(2:3), Hs=13 cm	P(3:7), Hs=14cm
0	0	11607.19	11740.61	12007.44	12007.44	12541.1
5	0.0177	12007.44	12140.86	12274.27	12274.27	12807.94
10	0.0354	12140.86	12274.27	12407.69	12407.69	12941.35
20	0.0708	12274.27	12541.1	12674.52	12674.52	13074.77
30	0.1062	12407.69	12674.52	12807.94	12807.94	13341.6
40	0.1415	12140.86	12407.69	12674.52	12941.35	13074.77
50	0.1769	12140.86	12407.69	12674.52	12807.94	13074.77
100	0.3539	12140.86	12407.69	12674.52	12807.94	13074.77
200	0.7077	12140.86	12407.69	12674.52	12807.94	13074.77
300	1.0616	12140.86	12407.69	12674.52	12807.94	13074.77
400	1.4154	12140.86	12407.69	12674.52	12807.94	13074.77
500	1.7693	12140.86	12407.69	12674.52	12807.94	13074.77

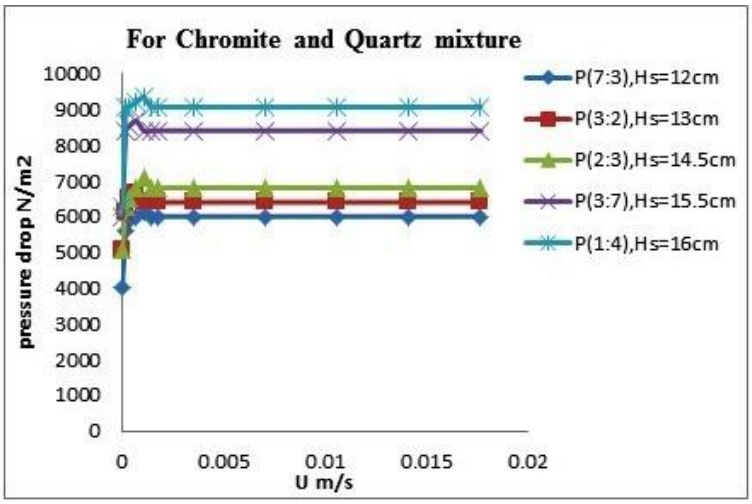

Fig.4.2. Variation of bed pressure drop with superficial water velocity for different weight ratio and stagnant bed height of chromite and quartz mixtur

Table 4.2

Effect of different weight ratio and stagnant bed height of binary mixture of chromite ore and quartz on pressure drop

Flow rate	Superficial velocity	Pressure drop across the bed N/m^2 (Chromite : Quartz)				
Q lit/hr.	U cm/s	P(7:3), Hs=12cm	P(3:2), Hs=13cm	P(2:3), Hs=14.5cm	P(3:7), Hs=15.5cm	P(1:4), Hs=16cm
0	0	4002.48	5069.808	5069.808	6003.72	6270.552
5	0.0177	5603.472	6137.136	6270.552	8405.208	9072.288
10	0.0354	5870.304	6537.384	6537.384	8538.624	9072.288
20	0.0708	6003.72	6670.8	6804.216	8672.04	9205.704
30	0.1062	6137.136	6403.968	7071.048	8405.208	9339.12
40	0.1415	6003.72	6403.968	6804.216	8405.208	9072.288
50	0.1769	6003.72	6403.968	6804.216	8405.208	9072.288
100	0.3539	6003.72	6403.968	6804.216	8405.208	9072.288
200	0.7077	6003.72	6403.968	6804.216	8405.208	9072.288
300	1.0616	6003.72	6403.968	6804.216	8405.208	9072.288
400	1.4154	6003.72	6403.968	6804.216	8405.208	9072.288
500	1.7693	6003.72	6403.968	6804.216	8405.208	9072.288

4.3.2 BED EXPANSION RATIO

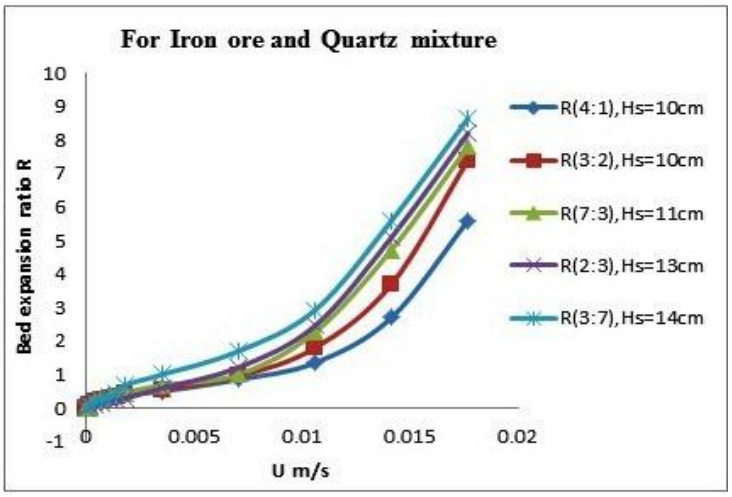

Fig.4.3. Variation of bed expansion ratio with superficial water velocity for different weight ratio and stagnant bed height of iron ore and quartz mixture

Table -4.3

Effect of different weight ratio and stagnant bed height of binary mixture of chromite and quartz on bed expansion

Flow rate	Superficial velocity	Bed Expansion ratio (Chromite : Quartz)				
Q lit/hr.	U cm/s	R(7:3), Hs=12cm	R(3:2), Hs=13cm	R(2:3), Hs=14.5cm	R(3:7) ,Hs=15.5cm	R(1:4), Hs=16cm
0	0	0	0	0	0	0
5	0.0177	0	0	0	0.032	0.05
10	0.0354	0.01	0.03	0.034	0.065	0.09
20	0.0708	0.042	0.06	0.088	0.097	0.1
30	0.1062	0.09	0.102	0.122	0.129	0.1333
40	0.1415	0.1	0.12	0.16	0.194	0.2667
50	0.1769	0.14	0.18	0.206	0.226	0.4
100	0.3539	0.18	0.2	0.333	0.419	0.7333
200	0.7077	0.5	0.8	1.06	1.2	1.6
300	1.0616	1.4	1.8	2.06	2.226	2.6
400	1.4154	2.708	3	3.2	3.452	4.1
500	1.7693	4.083	4.8	4.999	5.194	5.8

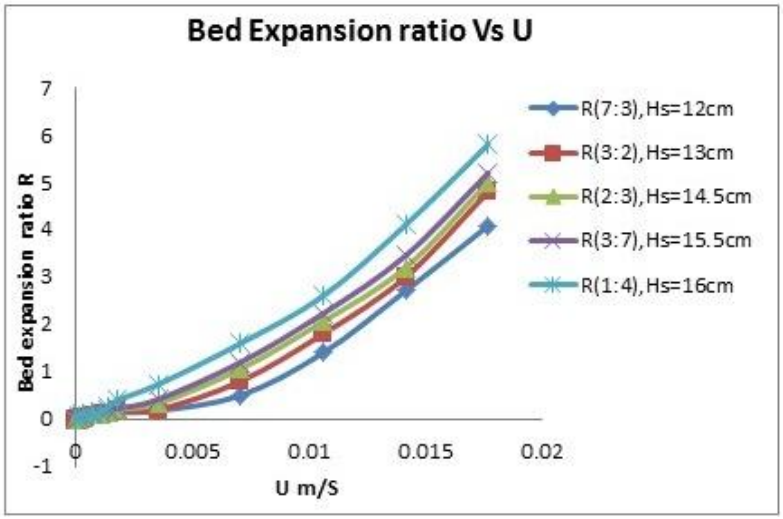

Fig.4.4. Variation of bed expansion ratio with superficial water velocity for different weight ratio and stagnant bed height of chromite and quartz mixture

Table -4.4

Effect of different weight ratio and stagnant height of binary mixture of iron ore and quartz on bed expansion

Flow rate	Superficial velocity	Bed expansion ratio (Iron ore : Quartz)				
Q lit/hr.	U cm/s	R(4:1), Hs=10cm	R(3:2), Hs=10cm	R(7:3), Hs=11cm	R(2:3), Hs=13cm	R(3:7) ,Hs=14cm
0	0	0	0	0	0	0
5	0.0177	0.1	0.1	0	0.036	0.107
10	0.0354	0.15	0.2	0.227	0.071	0.178
20	0.0708	0.2	0.25	0.273	0.143	0.25
30	0.1062	0.25	0.3	0.364	0.229	0.321
40	0.1415	0.3	0.35	0.409	0.236	0.429
50	0.1769	0.4	0.45	0.455	0.286	0.678
100	0.3539	0.5	0.55	0.682	0.593	1
200	0.7077	0.85	0.95	1	1.214	1.7
300	1.0616	1.35	1.8	2.273	2.462	2.928
400	1.4154	2.7	3.7	4.727	5.1	5.6
500	1.7693	5.6	7.4	7.8	8.2	8.643

From Fig.4.3 and Fig.4.4, shows the bed expansion ratio as a function of superficial velocity at different static bed height and wt.% of flotsam. If the static bed height increases, the bed expansion ratio increases. It has been observed that with the increase of superficial velocity expansion ratio of the bed increases gradually.

4.3.3 MIXING AND SEGREGATION

From the Table.4.5 it is shown that when the weight percentage of jetsam increases a large amount nearly 99% of jetsam collected in the bottom and 99% of flotsam in the top. Because in a large density difference, the separation of mixtures is easier. Again when the weight percentage of jetsam and flotsam is nearly close i.e., 50%:50% in the middle large amount of mixtures misplaced their position.

Table-4.5

Wt. % of iron ore and quartz

Height (cm)	wt.% of Iron ore and Quartz									
	(80:20)		(70:30)		(60:40)		(40:60)		(30:70)	
	jetsam	flotsam	jetsam	flotsam	jetsam	flotsam	jetsam	flotsam	jetsam	flotsam
75-100	2.4389	97.561	1.15	98.85	1.057	98.94	0.7192	99.280	0.15	99.85
50-75	13.013	86.986	10.55	89.45	2.485	97.515	1.2892	98.710	0.481	99.518
25-50	28.194	71.805	21.127	78.873	13.53	86.47	7.9873	92.012	2.970	97.029
0-25	93.593	6.4063	86.658	13.341	68.84	31.16	29.583	70.416	7.727	92.273

From the Table.4.6 it is shown that if the density difference between the two particles is not so large then it is difficult to separate or in other words misplacement of particles is high. In this table there is no clear separation between the chromite and quartz i.e., in the middle large amount of of particle s are misplaced. In the both cases, it is observed that iron ore and quartz mixture easily separate but in the case on chromite and quartz mixture not difficult to separate but large amount of materials are mixed. Hence if the density difference between the two materials is large then it is clear separation.

Table-4.6

Wt. % of chromite and quartz

Height (cm)	wt.% of Chromite and Quartz									
	(70:30)		(60:40)		(40:60)		(30:70)		(20:80)	
	jetsam	flotsam	jetsam	flotsam	jetsam	flotsam	jetsam	flotsam	jetsam	flotsam
75-100	7.075	92.925	5.0749	94.925	4.6051	95.395	1.17	98.83	1.15	98.85
50-75	10.16	89.838	8.9665	91.034	7.162	92.838	4.85	95.15	3.53	96.47
25-50	20.15	79.848	16.775	83.224	15.25	84.75	11.152	88.847	10.42	89.58
0-25	77.97	22.034	62.64	37.36	42.897	57.102	38.897	61.102	21.98	78.02

4.3.4 WT. % OF JETSAM VS. HEIGHT

Table -4.7

Effect of weight ratio on the jetsam distribution along the expanded bed height for iron ore and quartz mixture

Height (cm)	wt. % jetsam Iron ore : Quartz				
	(80:20)	(30:70)	(40:60)	(60:40)	(70:30)
75-100	2.4389	0.15	0.7192	1.0575	1.15
50-75	13.0138	0.4815	1.2892	2.485	10.55
25-50	28.1947	2.9703	7.9873	13.53	21.127
0-25	93.5937	7.727	29.5834	68.84	86.6585

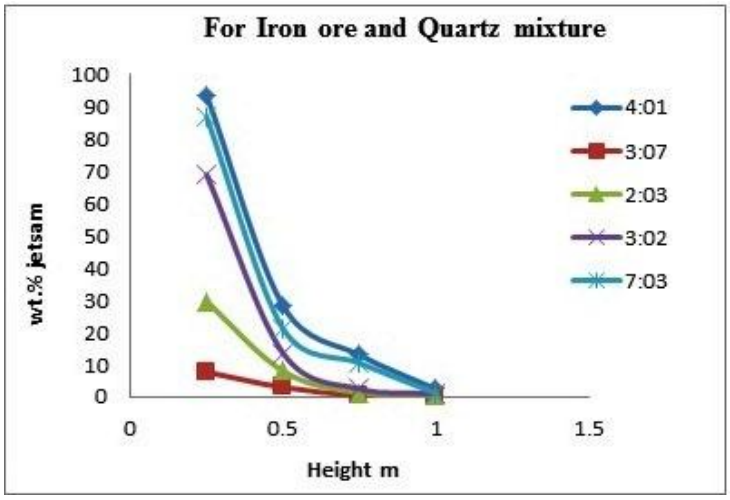

Fig.4.5. Wt % of jetsam Vs bed height for different ratio of iron ore and quartz mixture

From Fig.4.5 and Fig.4.6, shows the concentration of jetsam as a function of bed height at different percentages of jetsam in feed. From the experiment, we can observe that if the weight percentage of jetsam increases then the bed height decreases with respect to jetsam.

Table -4.8

Effect of weight ratio on the jetsam distribution along the expanded bed height for chromite and quartz mixture

Height	wt. % of jetsam Chromite : Quartz				
	(20:80)	(30:70)	(40:60)	(60:40)	(70:30)
75-100	1.15	1.17	4.6051	5.0749	7.0749
50-75	3.53	4.85	7.162	8.9665	10.162
25-50	10.42	11.1524	15.25	16.7753	20.1524
0-25	21.98	38.8975	42.8975	62.64	77.966

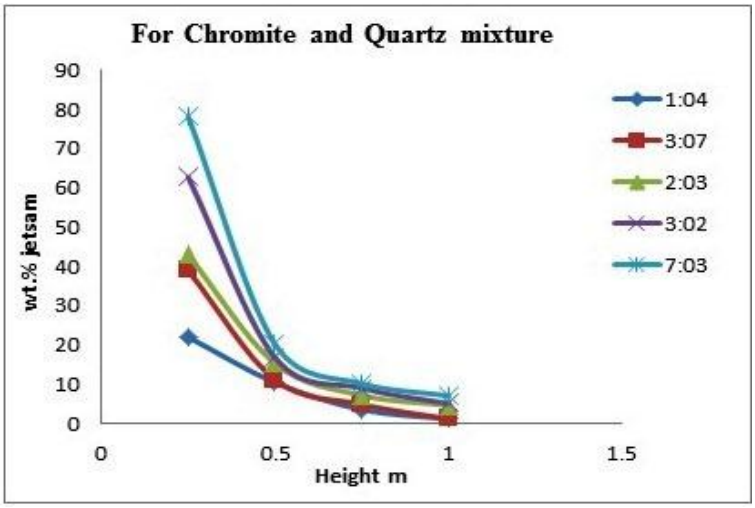

Fig.4.6 wt. % of jetsam vs. bed height for different ratio of chromite and quartz mixture

4.3.5 OVERALL BED VOIDAGES VS. SUPERFICIAL LIQUID VELOCITY

Bed expansion is depends on another parameter i.e.; over all bed voidage. From the Fig.4.7 and Fig.4.8 represents if the overall bed voidage is a function of superficial liquid velocity. Fig.4.7 and Fig.4.8 shows that the superficial water velocity increases than the expansion of the bed height is also increases for different weight ratio of flotsam and jetsam.

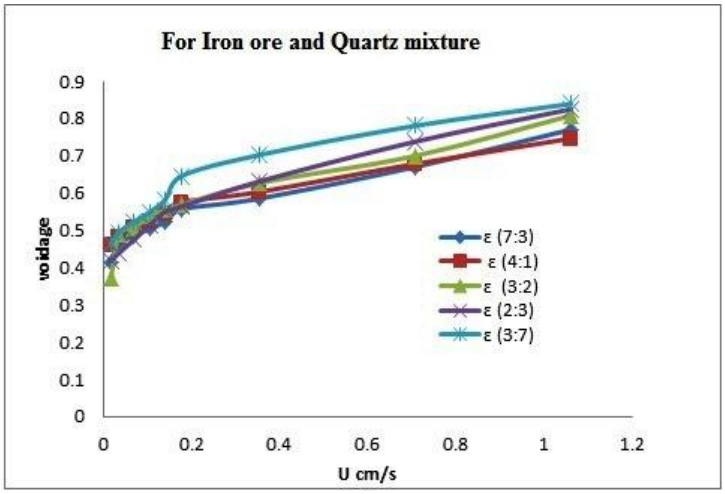

Fig.4.7 Variation of overall bed voidage with superficial water velocity for different ratio of iron ore and quartz mixture

Table -4.9

Effect of overall voidage along the expanded bed height for iron ore and quartz mixture

superficial liquid velocity cm/s	voidage of iron ore : quartz mixture				
U	ε (70:30)	ε (80:20)	ε (60:40)	ε (40:60)	ε (30:70)
0.0177	0.415872	0.459198	0.372545	0.418134	0.462465
0.0354	0.464549	0.482711	0.48874	0.438915	0.495043
0.0707	0.485967	0.504265	0.507	0.47632	0.523898
0.1061	0.505738	0.524095	0.539866	0.515111	0.549633
0.1415	0.524044	0.542399	0.554709	0.551132	0.58341
0.1768	0.556868	0.575084	0.568625	0.5636	0.645456
0.3537	0.585457	0.603412	0.626919	0.631211	0.702436
0.7074	0.670492	0.678442	0.699913	0.73816	0.780742
1.061	0.770521	0.746859	0.808278	0.82544	0.839773
1.415	0.863289	0.839221	0.890444	0.896642	0.905321
1.7683	0.923507	0.909866	0.928845	0.93454	0.938283

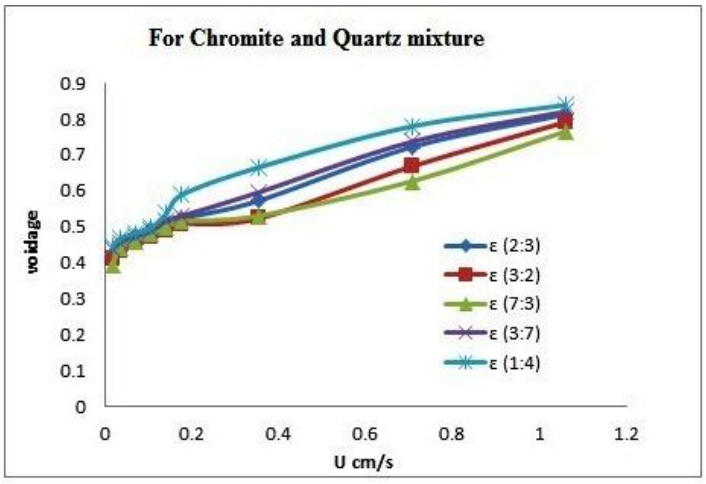

Fig.4.8 Variation of overall bed voidage with superficial water velocity for different ratio of iron ore and quartz mixture

Table -4.10

Effect of overall voidage along the expanded bed height for chromite and quartz mixture

superficial liquid velocity cm/s	voidage of chromite and quartz mixture				
U	ε (40:60)	ε (60:40)	ε (70:30)	ε (30:70)	ε (20:80)
0.0177	0.42465	0.41284	0.393473	0.438882	0.444658
0.0354	0.443828	0.434587	0.440129	0.456417	0.467525
0.0707	0.478589	0.45478	0.460865	0.472889	0.482739
0.1061	0.494389	0.473581	0.48012	0.488393	0.497107
0.1415	0.50926	0.491128	0.498047	0.516815	0.535791
0.1768	0.523281	0.507544	0.514778	0.529874	0.588542
0.3537	0.572176	0.522933	0.530431	0.595473	0.664738
0.7074	0.721914	0.668127	0.626753	0.736445	0.779218
1.061	0.812526	0.790875	0.765215	0.820674	0.838356
1.415	0.863236	0.85321	0.848368	0.870189	0.886849
1.7683	0.902993	0.899565	0.889722	0.909403	0.91379

4.4 CONCLUSION

In this chapter, it is observed that the bed expansion for the mixture increases with increase in the weight fraction of flotsam in the mixture. For any given fluidizing medium, a mixing/segregation regime map can be drawn in terms of size ratio and density ratio of the particles. The bed expansion ratio is increases with increase in weight ratio flotsam. Liquid-solid system is the one process for segregation of particles having different in their density. It has been observed that bed expansion can be used as an important indicator for the misplacement of particles in a column and the component density ratio of the mixture is a variable that affects the segregation pattern of binary bed. Irrespective of the density ratio of its components, the fluidization velocity interval of any two density mixture exhibits the same type of dependence on composition.

CHAPTER-5

CFD SIMULATION OF HYDRODYNAMIC CHARACTERISTIC OF BINARY MIXTURE

CHAPTER-5

CFD SIMULATION OF HYDRODYNAMIC CHARACTERISTIC OF BINARY MIXTURE

5.1 CFD (COMPUTATIONAL FLUID DYNAMICS)

Computational fluid dynamics is the branches of fluid mechanics which uses in numerical methods and algorithms to solve and analyze the fluid flows problems. Computers easy to solve the millions of calculations which required simulating the interaction of fluids and gases with the complex surfaces. However, it also simplified equations and high speed supercomputers, because only approximate solutions can be achieved in many cases. More accurate the codes that can accurately and quickly simulate even complex scenarios such as supersonic or turbulent flows are an ongoing area of research.

CFD is a powerful technique for the prediction of the fluid dynamics in various types of systems, thus, enabling a proper design of such systems. It is a sophisticated way to analyze not only for fluid flow behaviour but also the processes of heat and mass transfer. The availability of advanced commercial computational fluid dynamics (CFD) software and of faster computer processors has revolutionized scientific research in the field of multiphase flow. In the field of fluidization, in particular, the use of CFD is the fundamental understanding of fluid–solid interactions and enabled the correct theoretical prediction of various macroscopic phenomena encountered in fluidized beds. As regards to mathematical modeling, computational fluid dynamic (CFD) simulations of the flow in fluidized beds gives very detailed information about the local values of phase holdups and their three-dimensional distributions, liquid phase flow patterns and the intermixing levels of the individual phases especially in the regions where measurements are either difficult or impossible to obtain. So CFD useful for understanding of the transport phenomena in fluidized beds. The CFD modeling of fluidized beds can be classified into Eulerian–Lagrangian and Eulerian–Eulerian approaches. Eulerian–Lagrangian models describe the fluid flow using the continuum equations, and the particulate phase flow is described by tracking the motion of individual particles, but due to the computational limitations, the Eulerian–Lagrangian models are normally limited to a relatively small number of particles.

Therefore, the other approach, Eulerian–Eulerian continuum modelling, in which fluid and solid phases are treated as interpenetrating continuum phases. (Ding and Gidaspow, 1990).

5.2 ADVANTAGES OF CFD

Gas-solid multiphase flow modeling offer substantial process improves process plant operations. Now day, computational fluid dynamics (CFD) software developers focused on developing new model that can simulate liquid-solid flows to a much higher level of consistency. As a result, process industry engineers improve the model by evaluating alternatives methods but it is too expensive or time-consuming to trial on the plant floor. Previously, CFD has been used to improve process design by allowing engineers to simulate the model configurations, eliminating estimation that would normally be used to create model geometry and process conditions. The use of CFD helpful to engineers for obtaining solutions problem regarding complex geometry and boundary conditions. A CFD analysis applicable for pressure, fluid velocity, temperature, and species or phase concentration on a computational grid throughout the solution domain.

5.3 CFD MODELING OF MULTIPHASE SYSTEMS

There are some examples of multiphase systems:

- Absorbers, aeration, air lift pumps, cavitation, evaporators, scrubbers are the examples of bubbly flow
- Absorbers, combustors, dryers, evaporation, gas cooling, scrubbers are droplet flow.
- Large bubble motion in pipes or tanks is slug flow.
- Air classifiers,cyclone separators, dust collectors are particle-laden flow.
- Grains, transport of cement,and metal powders are pneumatic transport.
- Fluidized bed , circulating fluidized beds are fluidized bed.
- Slurry transport, mineral processing are slurry flow examples.
- Mineral processing, biomedical and physiochemical fluid systems are hydro transport.
- Mineral processing are sedimentation.

5.4 DISADVANTAGES OF CFD

- Physical models: The CFD solutions can only be as accurate as the physical models on which they are based.
- Numerical errors: numerical error when a probleme is solving in a computer
- Boundary conditions: when the initial/boundary conditions provided to the numerical model accurate then the CFD solution is as good as possible

5.5 APPLICATION OF COMPUTATIONAL FLUID DYNAMICS (CFD)

CFD is used for predicting the numerical results, when fluid flows, in operations involving simultaneous flow of heat, mass transfer, phase change (e.g. melting, freezing), chemical reactions(e.g. combustion), mechanical movement(e.g. piston ,fans), stress & displacement etc. Examples of CFD applications in the chemical process industry include separation, , mass transfer,heat exchange reaction, mixing,drying,pipeline flow,combustion, multiphase systems and material processing. Computational fluid dynamics (CFD) is the most promising for future fluidized bed for various modeling tools. With increasing computational capabilities and computational fluid dynamics (CFD) tools in recent years,study of the hydrodynamics of fluid-solid systems would be useful in the design, optimization and scale-up process. The predictive simulations using CFD make modeling more accurate and faster. Conventional scaling laws can be used to design a fluidized bed, either larger or smaller, with hydrodynamic similarity. However, similarity of mixing and segregation phenomena is not guaranteed. Hence simulation becomes the only potential tool useful for scaling fluidized beds used for fluidization of multi-component systems. The expanded bed height is depends on different variables like pressure drop, superficial velocity, bed height, overall bed voidage, volume fraction of the mixture etc.

5.6 APPROACHES TO MULTIPHASE MODELING

There are two approaches for the numerical calculation of multiphase flow model which is describe in the following section.

- Euler-Lagrange approach
- Euler-Euler approach

5.6.1 THE EULER-LAGRANGE APPROACH

The Lagrangian discrete phase model follows the Euler-Lagrange approach. The fluid phase is treated as a continuum by solving the time-averaged Navier-Stokes equations, while the dispersed phase is solved by tracking a large number of particles, bubbles, or droplets through the calculated flow field. The dispersed phase can exchange momentum, mass and energy with the fluid phase. This makes the model appropriate for the modeling of spray dryers, coal and liquid fuel combustion, and some particle laden flows, but inappropriate for the modeling of liquid-liquid mixtures, fluidized beds or any application where the volume fraction of the second phase is not negligible.

5.6.2 THE EULER-EULER APPROACH

In the Euler-Euler approach the different phases are treated mathematically as interpenetrating continua. Since the volume of a phase cannot be carried occupied by the other phases, the concept of the volume fraction is introduced. These volume fractions are assumed to be continuous functions of space and time and their sum is equal to one. Conservation equations for each phase are derived to obtain a set of equations, which have similar structure for all phases. These equations are closed by providing constitutive relations that are obtained from empirical information or in the case of granular flows by application of kinetic theory.

There are three different Euler-Euler multiphase models.

- Volume of fluid (VOF) model
- Mixture model
- Eulerian model.

.5.6.2.1 The VOF Model

The VOF model is a surface-tracking technique applied to a fixed Eulerian mesh. It is designed for two or more immiscible fluids where the position of the interface between the fluids is of interest. In the VOF model, a single set of momentum equations is shared by the fluids and the volume fraction of each of the fluids in each computational cell is tracked throughout the domain. The applications of VOF model include stratified flows, free surface flows, filling, sloshing, and the motion of large bubbles in a liquid.

5.6.2.2 The Mixture Model

The mixture model is designed for two of more phases (fluid or particulate). As in the Eulerian model, the phases are treated as interpenetrating continua. The mixture model solves for the mixture momentum equation and prescribes relative velocities to describe the dispersed phase. Applications of the mixture model include particle-laden flows with low loading, bubbly flows, and sedimentation and cyclone separators. The mixture model can also be used without relative velocities for the dispersed phase to model homogenous multiphase flow.

5.6.2.3 The Eulerian Model

The Eulerian model is the most complex of the multiphase models. It solves a set of N momentum and continuity equations for each phase. Couplings are achieved through the pressure and inter phase exchange coefficients. The manner in which this coupling is handled depends upon the type of phases involved; granular (fluid-solid) flows are handled differently than non-granular (fluid-fluid) flows. For granular flows, the properties are obtained from application of kinetic theory. Momentum exchange between the phases is also dependent upon the type of mixture being modeled. Applications of the Eulerian Multiphase Model include bubble columns, risers, particle suspension, and fluidized beds.

5.7 CHOOSING A MULTIPHASE MODEL

The first step in solving any multiphase problem is to determine which of the regimes best represent the flow. General guidelines provides some broad guidelines for determining the appropriate models for each regime, and detailed guidelines provides details about how to determine the degree of interphase coupling for flows involving bubbles, droplets or particles, and the appropriate models for different amounts of coupling. In general, once that the flow regime is determined, the best representation for a multiphase system can be selected using appropriate model based on following guidelines (Fluent doc., 2006). Additional details and guidelines for selecting the appropriate model are:

- For bubble, droplet and particle-laden flows in which dispersed-phase volume fractions are less than or equal to 10% use the discrete phase model.
- For slug flow, use the VOF model.

- For stratified / free-surface flows, use the VOF model.
- For pneumatic transport use the mixture model for homogenous flow or the Eulerian Model for granular flow.
- For fluidized bed, use the Eulerian Model for granular flow.
- For slurry flows and hydro transport, use Eulerian or Mixture model.
- For sedimentation, use Eulerian Model.

5.8 COMPUTATIONAL FLOW MODEL

In the present work, an Eulerian multi-fluid model is adopted where liquid and solid phases are all treated as continua, inter- penetrating and interacting with each other everywhere in the computational domain. The pressure field is assumed to be shared by all three phases, in proportion to their volume fraction. The motion of each phase is governed by respective mass and momentum conservation equations.

5.8.1 GOVERNING EQUATIONS

Continuity Equation:

$$\frac{\partial}{\partial t}(\varepsilon_k \rho_k) + \nabla.(\varepsilon_k \rho_k u_k) = 0 \quad (5.1)$$

Where ρ_k is the density and ε_k is the volume fraction of phase k= s, l and the volume fraction of the phases satisfy the following condition:

$$\varepsilon_l + \varepsilon_s = 1 \quad (5.2)$$

Momentum Equations:

For liquid phase:

$$\frac{\partial}{\partial t}(\varepsilon_l \rho_l u_l) + \nabla.(\varepsilon_l \rho_l u_l u_l) = -\varepsilon_l \nabla P + \nabla.\tau_l + \rho_l \varepsilon_l g_l + F_{i,l} \quad (5.3)$$

For solid phase:

$$\frac{\partial}{\partial t}(\varepsilon_s \rho_s u_s) + \nabla.(\varepsilon_s \rho_s u_{si} u_{si}) = -\varepsilon_s \nabla P - \nabla P_s + \nabla.\tau_s + \rho_s \varepsilon_s g_s + F_{i,s} \quad (5.4)$$

Where ∇P is the pressure shared by all phases. The second term on the R.H.S of solid phase momentum Eq. (5.4) is the term that accounts for additional solid pressure due to solid collisions. The terms $F_{i,l}$ and $F_{i,s}$ of the above momentum equations represent the interphase momentum exchange term for liquid and solid phase, respectively.

The terms τ_l and τ_s in Equations (5.3) and (5.4) are the stress-strain tensors of liquid and solid phase, respectively and are defined as;

$$\tau_l = \varepsilon_l \mu_l (\nabla u_l + \nabla u_l^T) + \varepsilon_l \left(\lambda_l - \frac{2}{3}\mu_l\right) \nabla . u_l I$$

$$\tau_s = \varepsilon_s \mu_s (\nabla u_s + \nabla u_s^T) + \varepsilon_s \left(\lambda_s - \frac{2}{3}\mu_s\right) \nabla . u_s I$$

Where μ_l and μ_s are the shear viscosity and λ_l and λ_s are the bulk viscosity of liquid and solid phase, respectively.

5.8.2 TURBULENCE MODELING

To describe the effects of turbulent fluctuations of velocity and scalar quantities the simplest but complete model is the two-equation standard k-ε model. In comparison to single-phase flows, the number of terms to be modeled in the momentum equations in multiphase flows is large, and this makes the modeling of turbulence in multiphase simulations extremely complex. There are three methods for modeling turbulence in multiphase flows within the context of the k-ε model. Those are (a) mixture turbulence model, (b) dispersed turbulence model, and (c) turbulence model for each phase. In this work the k-ε dispersed turbulence model has been used for the turbulence modeling, as this model is applicable when there is clearly a primary continuous phase and the rest are dispersed secondary phases and seem to be the most probable model.

Additional transport equations for the turbulent kinetic energy k and its dissipation rate ε were considered: the standard k–ε model was chosen for modeling the turbulence. It has the properties such as robustness and reasonable accuracy for a wide range of industrial applications, with recently developed model improvements that provide better performance in the presence of jets and mixing layers.

The turbulence kinetic energy, k, and its rate of dissipation, ε, are obtained from the following transport equations:

$$\frac{\partial}{\partial t}(\rho k) + \frac{\partial}{\partial x_i}(\rho k u_i) = \frac{\partial}{\partial x_j}\left[\left(\mu + \frac{\mu_t}{\sigma_k}\right)\frac{\partial k}{\partial x_j}\right] + G_k + G_b - \rho\varepsilon - Y_M + S_k \quad (5.5)$$

$$\frac{\partial}{\partial t}(\rho\varepsilon) + \frac{\partial}{\partial x_i}(\rho\varepsilon u_i) = \frac{\partial}{\partial x_j}\left[\left(\mu + \frac{\mu_t}{\sigma_\varepsilon}\right)\frac{\partial \varepsilon}{\partial x_j}\right] + C_{1\varepsilon}\frac{\varepsilon}{k}(G_k + C_{3\varepsilon}G_b) - C_{2\varepsilon}\rho\frac{\varepsilon^2}{k} + S_\varepsilon \quad (5.6)$$

Where G_k represents the generation of turbulence kinetic energy due to the mean velocity gradients, G_b is the generation of turbulence kinetic energy due to buoyancy, Y_M represents the contribution of the fluctuating dilatation in compressible turbulence to the overall dissipation rate. $C_{1\varepsilon}$, $C_{2\varepsilon}$ and $C_{3\varepsilon}$ are constants. σ_k and σ_ε are the turbulent Prandtl numbers for k and ε, respectively. S_k and S_ε are user-defined source terms.

The turbulent (or eddy) viscosity, μ_t, is computed by combining k and ε as follows:

$$\mu_t = \rho C_\mu \frac{k^2}{\varepsilon} \quad (5.7)$$

Where Cμ is a constant.

5.8.3 DISCRETIZATION

ANSYS FLUENT uses a control-volume-based technique to convert the governing equations to algebraic equations that can be solved numerically. This control volume technique consists of integrating the governing equations about each control volume, yielding discrete equations that conserve each quantity on a control-volume basis (ANSYS FLUENT 13.0). In the current work Second Order Upwind discretization scheme is used to discretize momentum, turbulent kinetic energy and turbulent dissipation rate but for volume fraction First Order Upwind discretization scheme is used. In this scheme quantities at cell faces are determined by assuming that the cell-center values of any field variable represent a cell-average value and hold throughout the entire cell; the face quantities are identical to the cell quantities. The main advantage is that it is easy to implement and gives stable results with reasonable accuracy and takes less computational time (Fluent.13). For pressure-velocity coupling Semi-Implicit Method for Pressure-Linked Equations (SIMPLE) is used. It is one of the most commonly used methods. It is based on the premise that fluid flows from regions with high pressure to low pressure.

5.8.4 GEOMETRY AND MESH

ANSYS FLUENT 13.0 was used for making 2D rectangular geometry with width of 0.1m and height 1.5m. Mesh size of 0.0025 m was taken in order to have 49282 numbers of nodes and 24000 numbers of elements for the whole geometry in order to have better accuracy, which requires smaller time steps 0.001, more number of iterations per time step for the solution to converge. Fig.5.1 shows fine types of meshing.

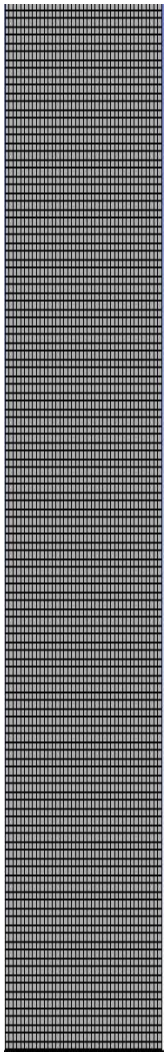

Fig.5.1 2D Mesh

5.8.5 SELECTION OF MODELS FOR SIMULATION

ANSYS FLUENT.13.0 was used for simulation. 2D segregated 1st order implicit unsteady solver is used (segregated solver must be used for multiphase calculations). Standard k-ε dispersed Eulerian multiphase model with standard wall functions were used. The model constants are tabulated as:

Table.5.1 Model constants used for simulation

Model Constants	Values
C_{mu}	0.09
C1-Epsilon	1.44
C2-Epsilon	1.92
C3-Epsilon	1.3
TKE Prandtl Number	1
TDR Prandtl Number	1.3
Dispersion Prandtl Number	0.75

Water is taken as continuous phase while binary mixtures are taken as dispersed phase. Interphase interactions formulations used were

Solid-Solid: Schiller-Naumann

Solid-Liquid: Gidaspow

Velocity Inlet Boundary Conditions: Water velocities ranging from 0.0177cm/s to 1.7683cm/s

Pressure outlet: 0 (atmospheric pressure)

5.8.6 BOUNDARY AND INITIAL CONDITIONS

In order to obtain a well-posed system of equations, reasonable boundary conditions for the computational domain have to be implemented. Inlet boundary condition is a uniform liquid velocity at the inlet, and outlet boundary condition is the pressure boundary condition, which is set as1.013×10^5 Pa. Wall boundary conditions are no-slip boundary conditions for the liquid phase and solid phase. The higher viscous effect and higher velocity gradient near the wall have been dealt with the standard wall function method. At initial condition, for iron ore volume fraction of 0.95 and for quartz 0.93 of the static bed height of column has been used.

5.8.7 SOLUTION CONTROLS

The solution procedure involves the different steps:

(i) Generation of suitable grid system;

(ii) Conversion of governing equation into algebraic equations;

(iii) Selection of discretization schemes;

(iv) Formulation of the discretized equation at every grid location;

(v) Formulation of pressure equation;

(vi) Development of a suitable iteration scheme for obtaining a final solution.

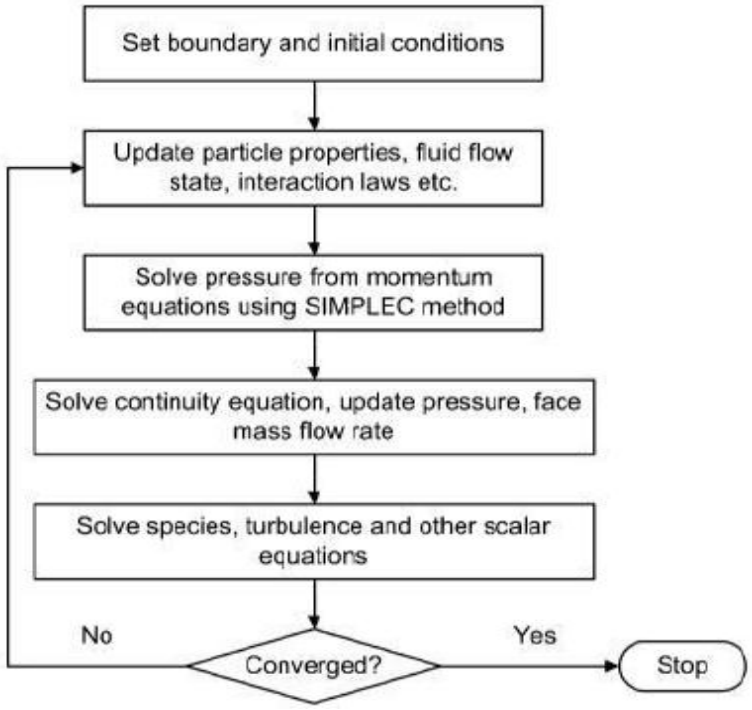

Fig.5.2 Flow diagram for the computational treatment of the equations

The Phase Coupled SIMPLE method (Patanker, 1980) has been chosen for pressure–velocity coupling. The second-order upwind scheme has been used for discretization of momentum, turbulence kinetic energy and turbulence dissipation rate and the first-order upwind scheme has been used for discretization of volume-fraction equations. The time step size of 0.001s has been used.

The following under relaxation factors have been used for different flow quantities: pressure=0.7, density = 1, body forces = 1, momentum = 0.1, volume fraction = 0.5, granular temperature = 0.2, turbulent kinetic energy = 0.8, turbulent dissipation rate = 0.8 and turbulent viscosity =1. The simulations have been carried out till the system reached the quasi-steady state i.e., the averaged flow variables are time independent; this can be achieved by monitoring the expanded bed height or phase volume fractions.

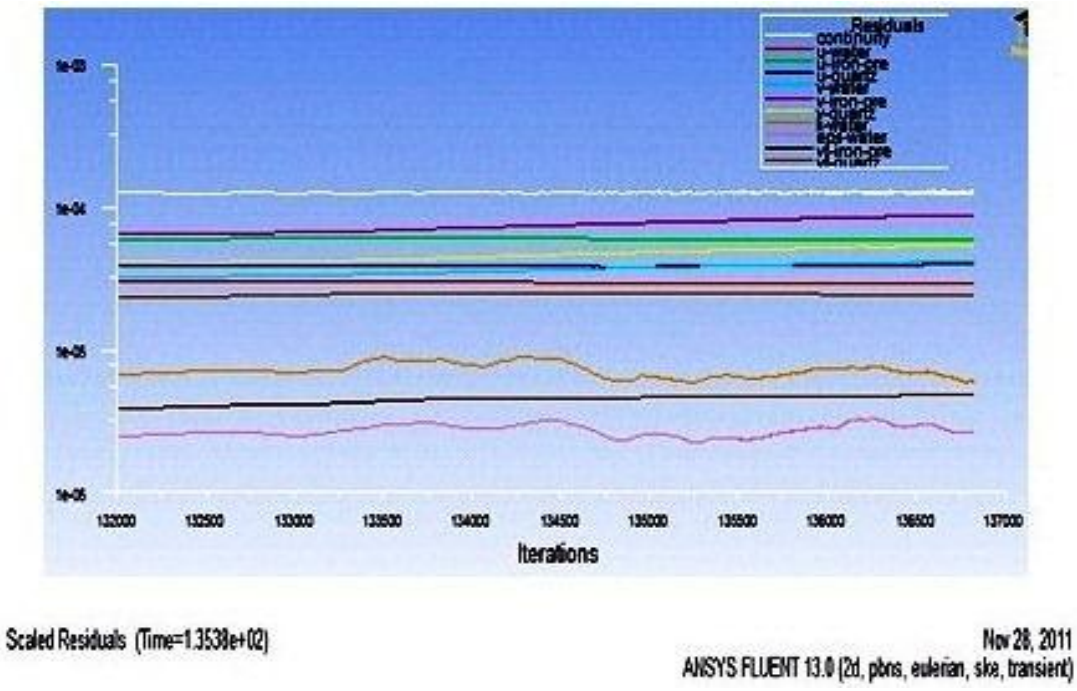

Fig. 5.3 Plot of residuals with the progress of simulation

The convergence criteria for all the numerical simulations are based on monitoring the mass flow residual and the value of 0.001 was set as converged value. The residual plot of the progress of the simulation is shown in Fig.5.3.

5.9 RESULTS AND DISCUSSIONS

5.9.1 CONTOURS OF VOLUME FRACTION OF SOLIDS

Fig. 5.4 and Fig.5.5 shows the variation in the bed profile with time for iron ore and quartz mixture and chromite and quartz mixture. It can be observed from the Fig.5.4 that, the bed profile is almost the same between 170 sec to 180 sec of simulation time. Simulations continued for 260sec. Here the contour plot is shown for every 10 sec difference time step. Similarly Fig.5.5 shows that the bed profile nearly same between 280 sec to 300 sec of simulation time but simulation is continued for 500 sec and the contour plot is shown for every 20 sec. While simulating the fluidized bed the bed profile changes with time. But after some time there is no significant change in bed profile. This indicates that the fluidized bed reached in a quasi-steady state. Once the fully developed quasi-steady state is reached, then calculate the averaged quantities in terms of time, axial and radial direction.

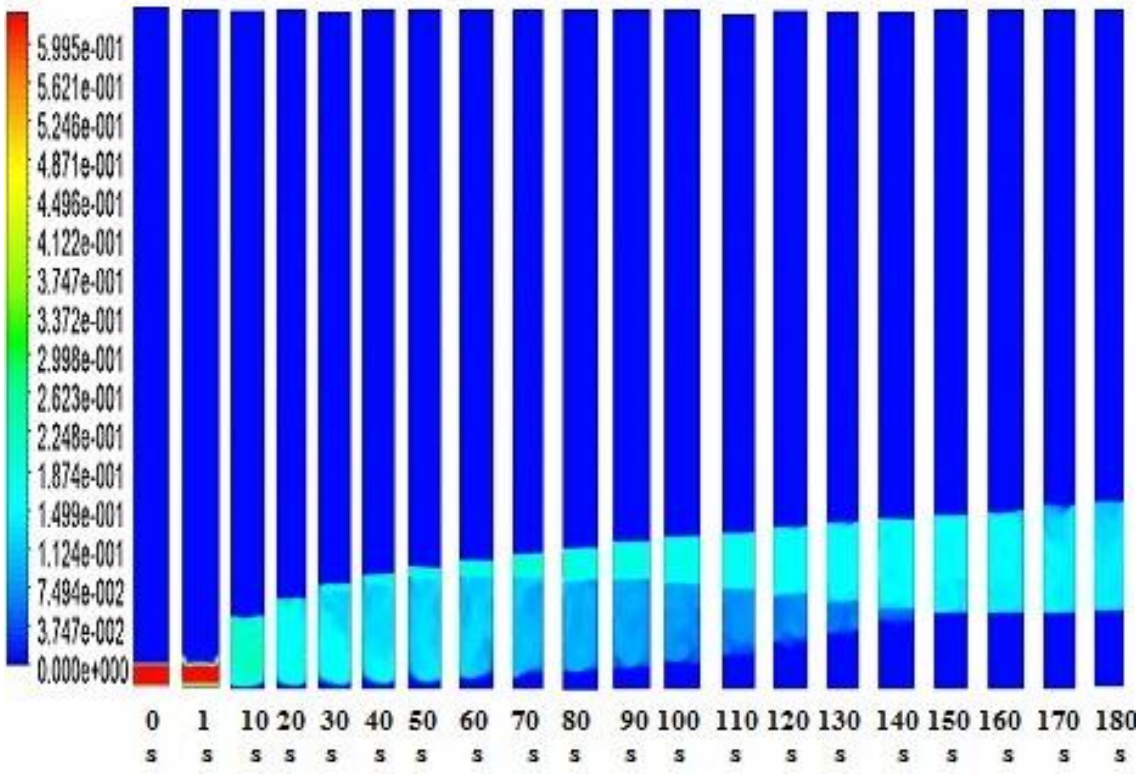

Fig. 5.4 Contours of volume fraction of 125µm quartz for Iron ore and Quartz mixture at water velocity of 0.007073 m/s with respect of time for initial bed height 0.1 m

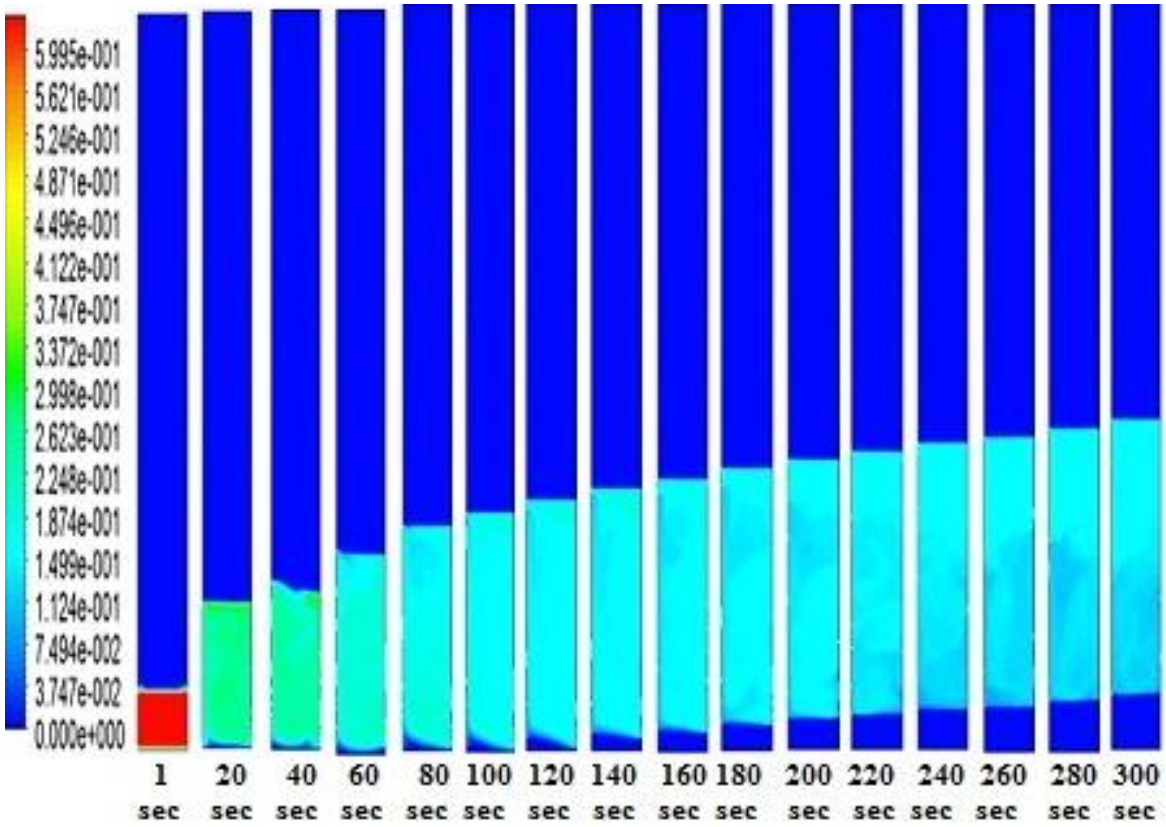

Fig. 5.5 Contours of volume fraction of 125µm quartz for Chromite and Quartz mixture at water velocity of 0.007073 m/s with respect of time for initial bed height 0.13 m

5.9.2 PHASE DYNAMICS

Solid and liquid phase dynamics have been represented in the form of contours, vectors and XY plots. Fig.5.6 shows the contours of volume fractions of iron ore, quartz and water in the column obtained at water velocity of 0.007073 m/s for initial static bed height 0.1 m and iron ore and quartz diameter 125 µm after the quasi steady state is achieved. Similarly Fig.5.7 shows that the contour of volume fraction of chromite, quartz and water at a water velocity of 0.007073 m/s for initial static bed height of 0.16 m. The colour scale given to the left of each contours gives the value of volume fraction corresponding to the colour. The contours for iron ore, chromite and quartz illustrates that bed is in fluidized condition. The contour for water illustrates that volume fraction of the liquid is less in fluidized section than the iron ore, chromite and quartz.

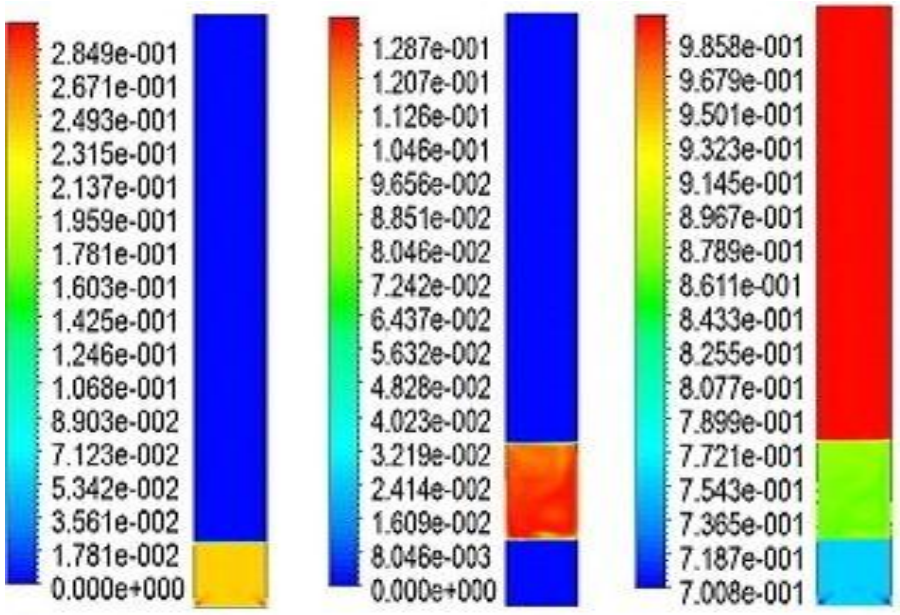

Iron ore **Quartz** **Water**

Fig. 5.6 Contours of volume fraction of iron ore, quartz, water at water velocity of 0.007073 m/s for initial static bed height of 0.1 m

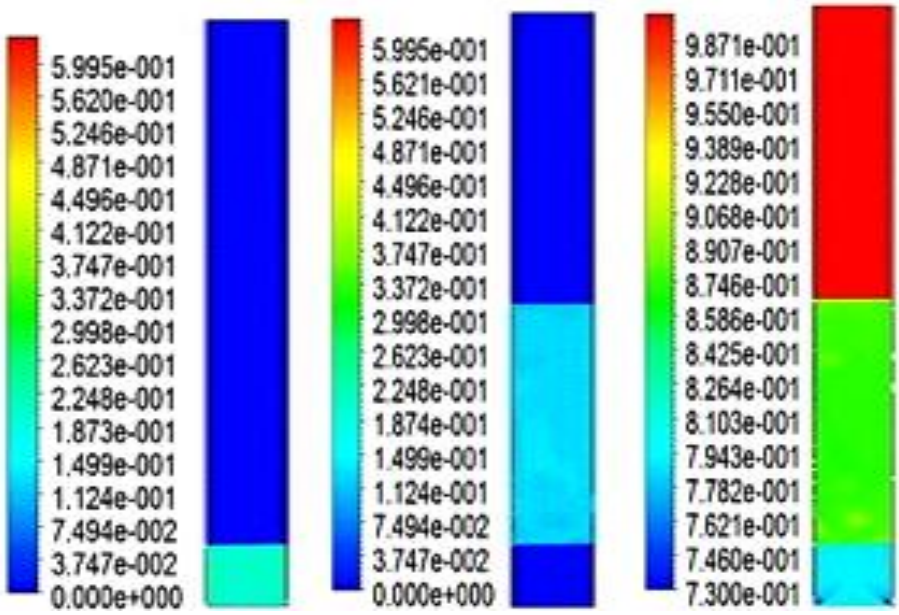

Chromite **Quartz** **Water**

Fig. 5.7 Contours of volume fraction of Chromite, quartz, water at water velocity of 0.007073 m/s for initial static bed height of 0.16 m

5.9.3 VELOCITY VECTOR OF SOLID AND LIQUID PHASES

Fig. 5.8 shows the velocity vectors of iron ore, quartz and water in the column obtained at water velocity of 0.000177 m/s for initial static bed height 0.1 m and iron ore and quartz of diameter size 125µm after the quasi steady state has been achieved. Similarly velocity vector of chromite, quartz and water shown in Fig.5.9 at water velocity of 0.007073 m/s for initial static bed height of 0.16 m. The velocity vectors are helpful in determining flow patterns in fluidized bed. From the vector of solids it can be seen that, there is a small length vigorous movement of the solid particles at the bottom part of the bed. In the upper part of the fluidizing section there is a circulatory motion of the particles with movement near the wall in the down ward direction while that in the central zone is upward. But in case of the velocity vector of water in the column shows always an upward trend. However the velocity is more in fluidized section of the bed compared to the part of the column which contains no solids. This is because less space is available for water to flow. The transition from high to low velocity can be clearly seen when water leaves fluidized part of the bed.

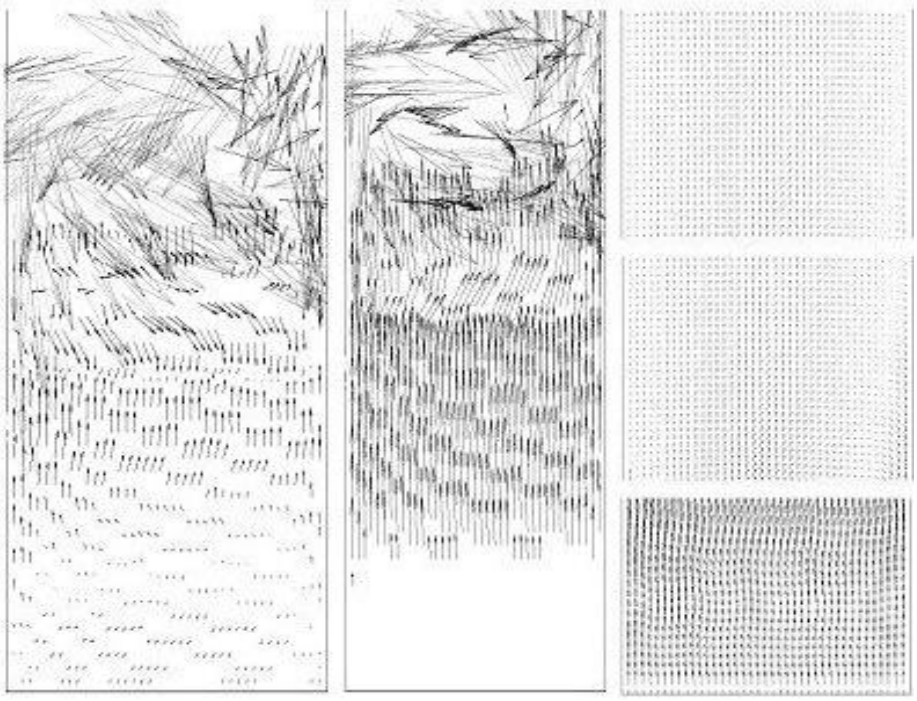

Iron Ore **Quartz** **Water**

Fig 5.8 Velocity vector of Iron ore, Quartz and Water

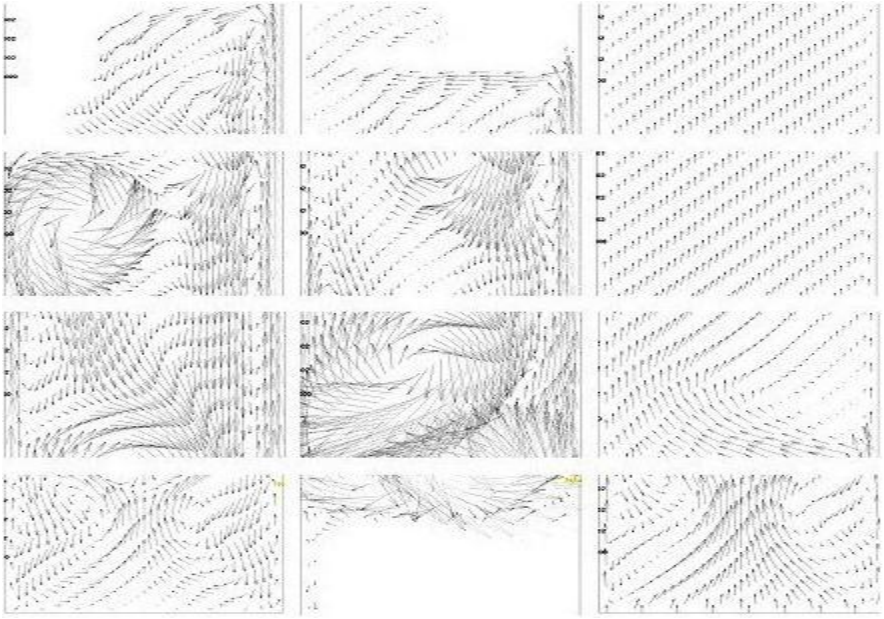

Chromite **Quartz** **Water**

Fig 5.9 Velocity vector of Chromite, Quartz and Water

5.9.4 RADIAL DISTRIBUTION OF AXIAL VELOCITY OF LIQUID PHASE

Fig. 5.10 shows that the XY plot for the radial distribution of axial velocity of liquid phase obtained from the simulation at an inlet water velocity of 0.001415 m/s for iron ore and quartz and chromite and quartz mixtures. This indicates a fully developed flow in the bed. The plots give a peak velocity of water of about 0.0015 m/s and 0.00155 m/s.

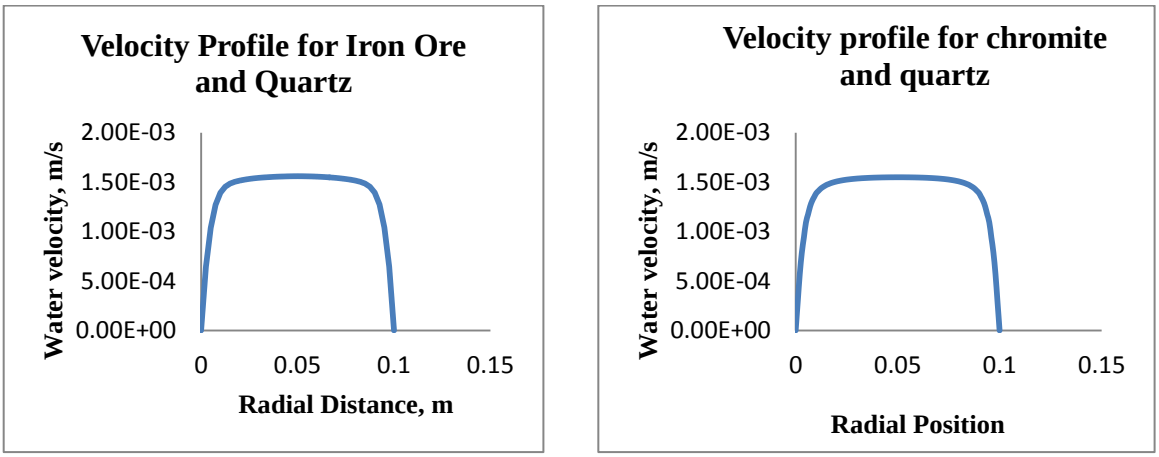

Fig.5.10 XY plot of velocity magnitude of liquid phase

5.9.5 BED EXPANSION (BED VOIDAGE)

In liquid-solid system with increase in liquid velocity, the expanded bed height increases and the voidage of the bed also increases. Experimentally this phenomenon has been observed for both iron ore and quartz mixture and chromite and quartz mixture in previous. CFD simulation result also shows an increase in bed expansion with liquid velocity. Fig. 5.11 and Fig.5.12 shows that the contours of solid volume fraction that there is steady increase in bed height with liquid velocity above the minimum fluidization condition.

The bed height can be determined from the XY plot of the iron ore, chromite and quartz volume fraction with respect to the axial distance from the base of the column (in 2D mesh it is noted as y-coordinate) as shown in Fig.5.13(iron ore and quartz mixture). The point where the solid fraction sharply decreases to zero value can be taken as the height of the bed.

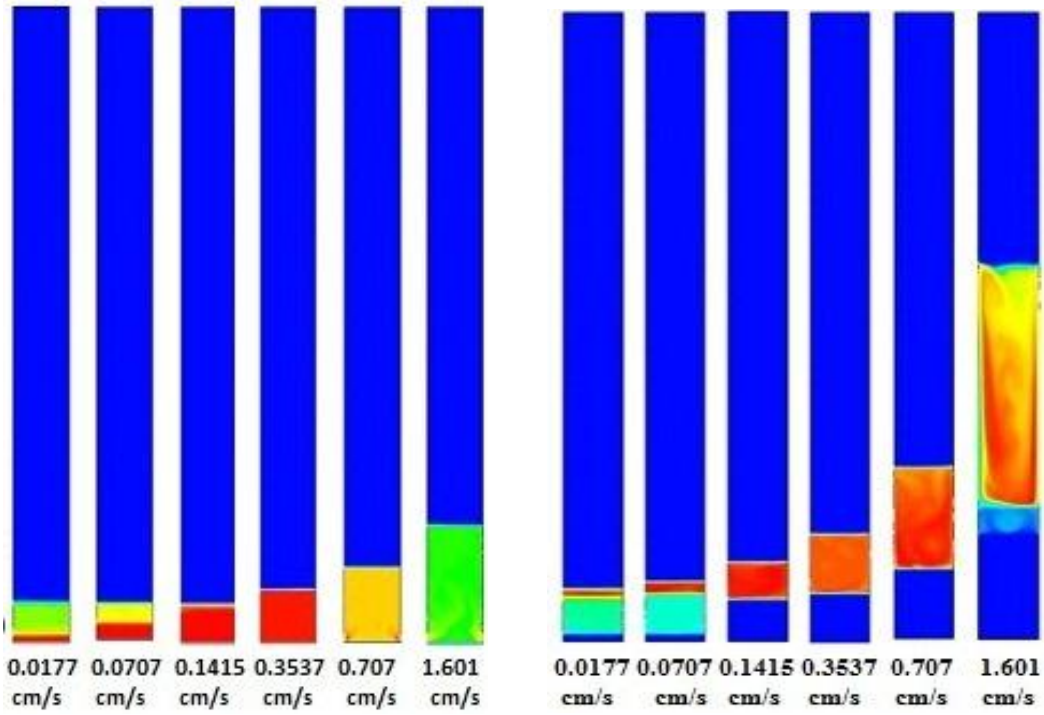

Fig. 5.11 Contour plot of iron ore and Quartz volume fraction with variation in liquid velocity

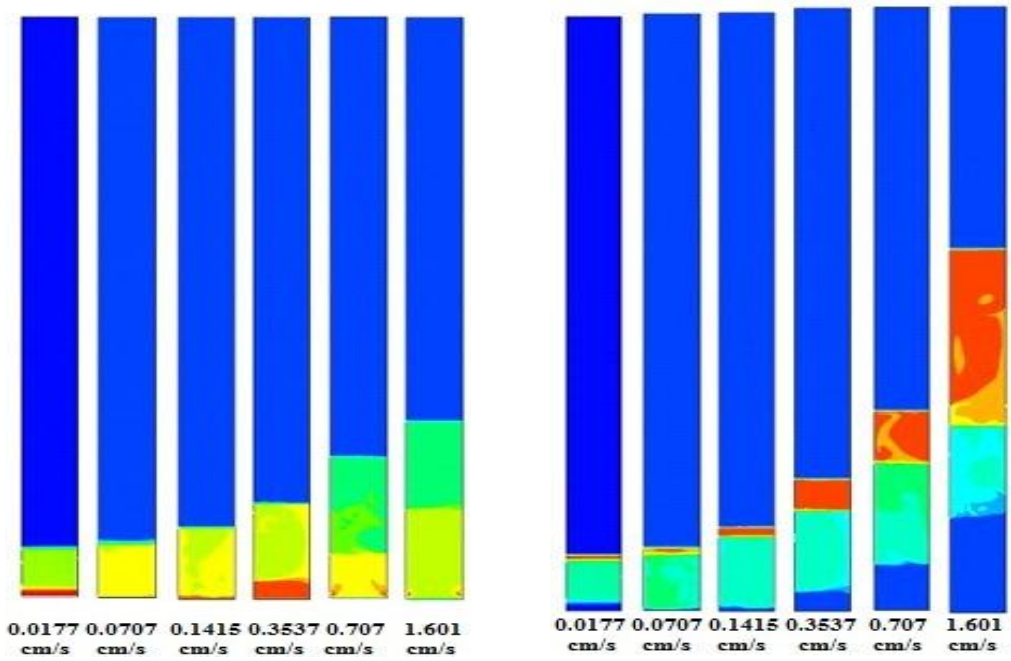

Fig. 5.12 Contour plot of Chromite and Quartz volume fraction with variation in liquid velocity

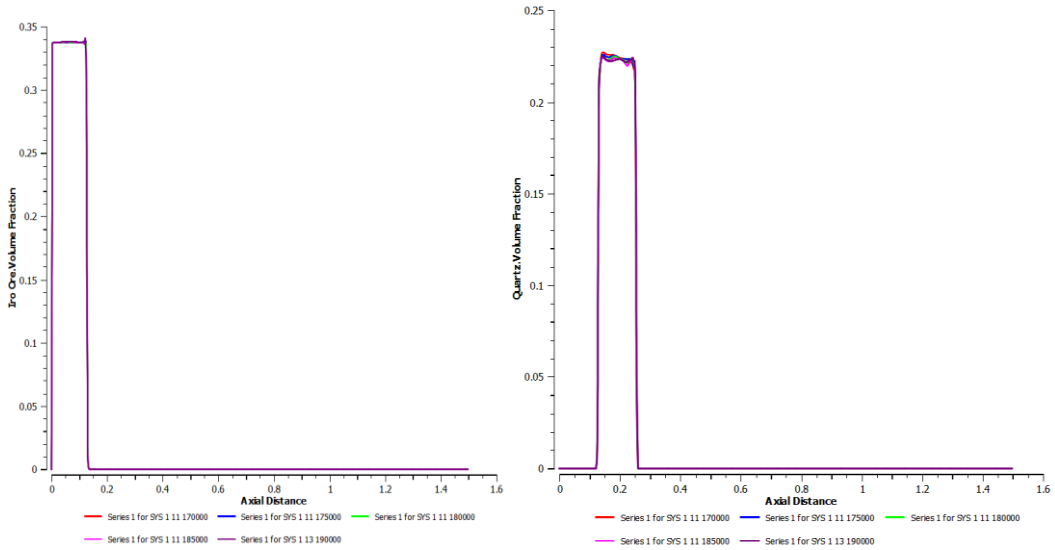

Fig. 5.13 XY plot of Iron ore and Quartz volume fraction

Fig.5.14 and Fig.5.15 shows the plot of simulated expanded bed height vs. liquid velocity and comparison between obtained simulated and experimental results. Bed height increases with increase in superficial velocity similar to the experimental results. It is also indicated from

comparison figure that there is slight decrease in the experimentally obtained expanded bed height in comparison to simulated expanded bed height with increase in the liquid velocity.

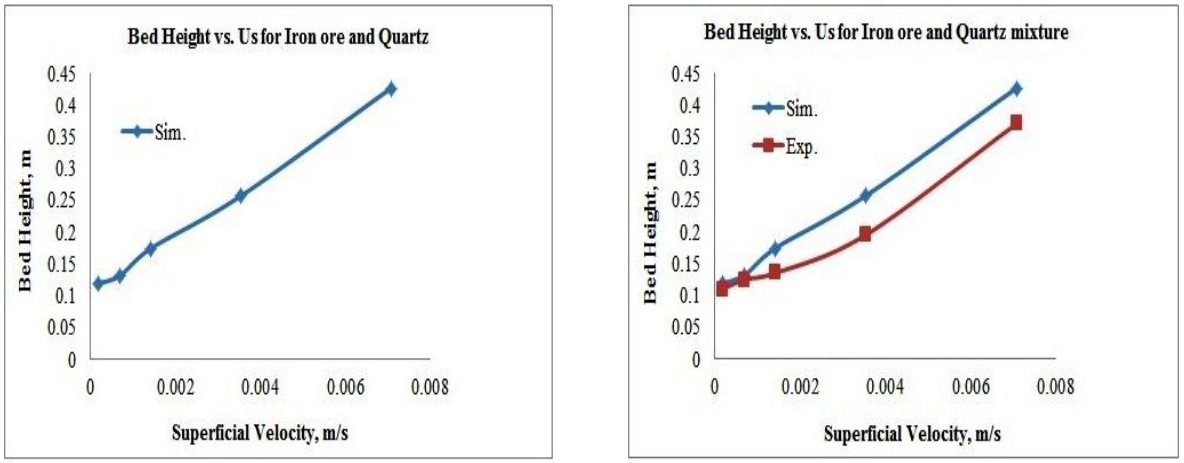

(a) **(b)**

Fig. 5.14 (a) CFD simulation of Bed expansion behaviour at Hs =0.1m (b) comparison of bed height obtained from simulated and the experimental values for iron ore and quartz mixture.

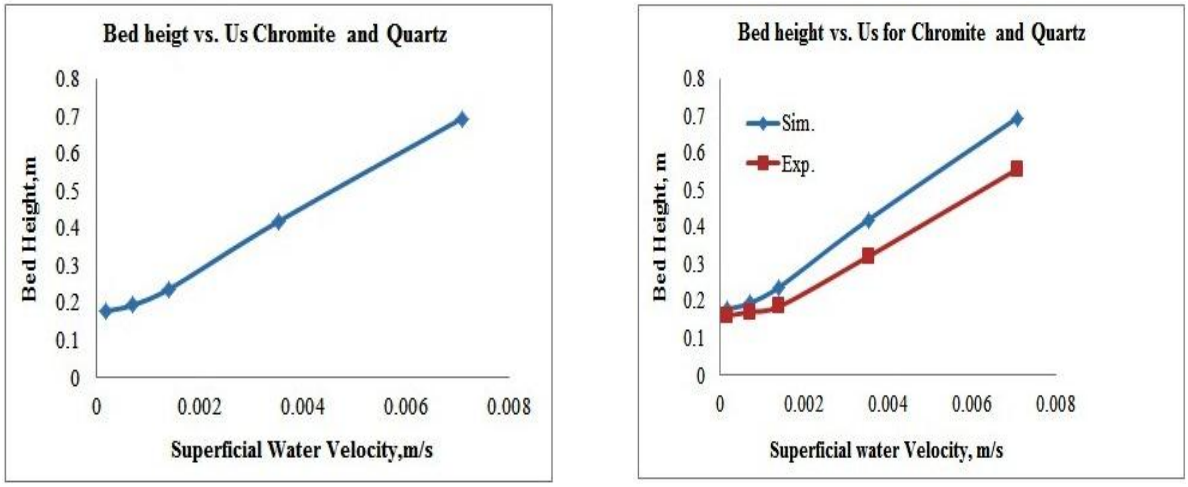

(a) **(b)**

Fig. 5.15 (a) CFD simulation of bed expansion behaviour at H*s*=0.16 m (b) comparison of bed height obtained from simulated and the experimental values for chromite and quartz mixture

Fig. 5.16 shows the plot of expanded bed height vs. superficial liquid velocity obtained at different weight ratio of iron ore and quartz mixture. It is indicated from figure that the simulated expanded bed height is increases with increase in the liquid velocity similar to the experimental results.

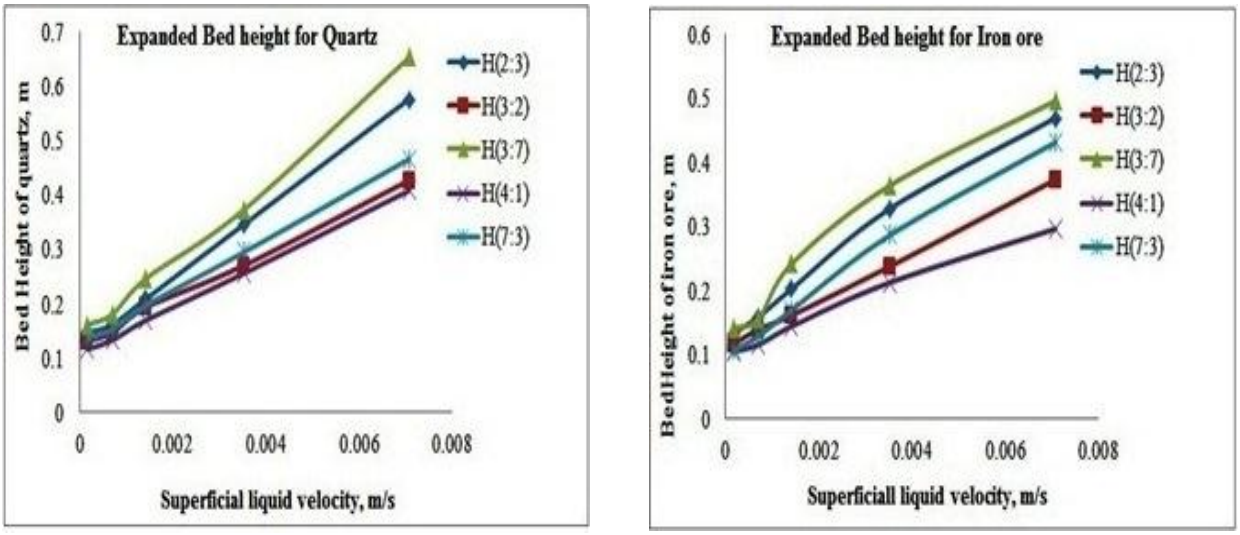

Fig. 5.16 CFD simulation result of expanded bed height vs. superficial liquid velocity at different weight ratio of iron ore and quartz mixture

Fig. 5.17 shows a comparison of the simulated and the experimental values of expanded bed height vs. superficial liquid velocity. A very good agreement is seen between the experimental and simulated values, but there is some deviation between both the values have been found. At this higher velocity the simulated bed height has been found to be higher than the experimental one. In experiment, increasing bed height has been observed with the increase in the liquid velocity. Simialarly increasing simulated bed height with increasing liquid velocity. Some investigator also study the comparison between experimental and simulation values and they found that there some variation between experimental and simulated values about 10%. In Fig. 5.17 at low liquid velocity, the simulated and experimental bed height has been good agreement occures with increase in liquid velocity.

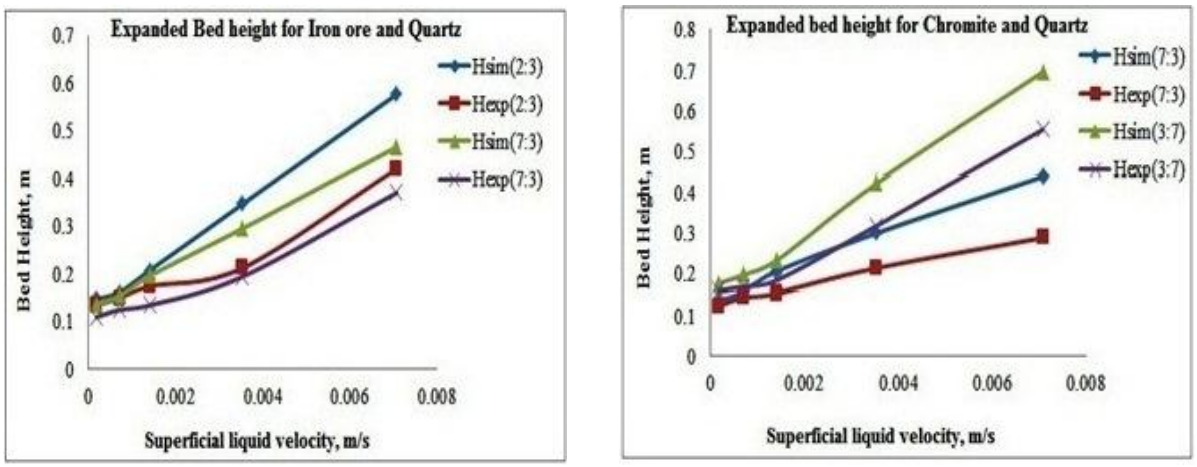

Fig. 5.17 Comparison of bed height vs. superficial liquid velocity obtained from experimental and CFD simulation

Fig.5.18 shows that mixing and segregation of iron ore and quartz mixture. Figure shows that the when the velocity is less there is the starting point of fluidized a bed of particles and is started to mix with each other and some amount of both the materials present in both upper and lower section of the fluidizing column. Therefore maximum amount of material clearly mixed in this velocity. Similarly when the velocity increases the materials are slowly separate with each other. At a velocity higher than fully fluidized velocity the materials are either segregates or mixed. So in this figure velocity 0.007073 m/s both the lighter and heavier material completely segregate with each other. This is because of density difference between the two materials are higher.

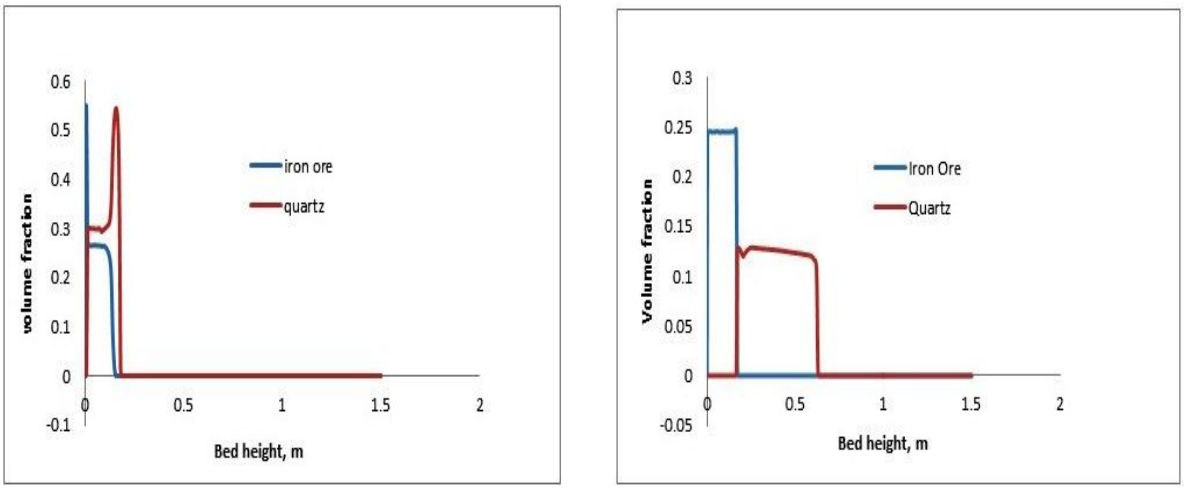

Fig. 5.18 mixing and segregation at a velocity 0.000707 m/s and 0.007073 m/s results obtain from CFD simulation

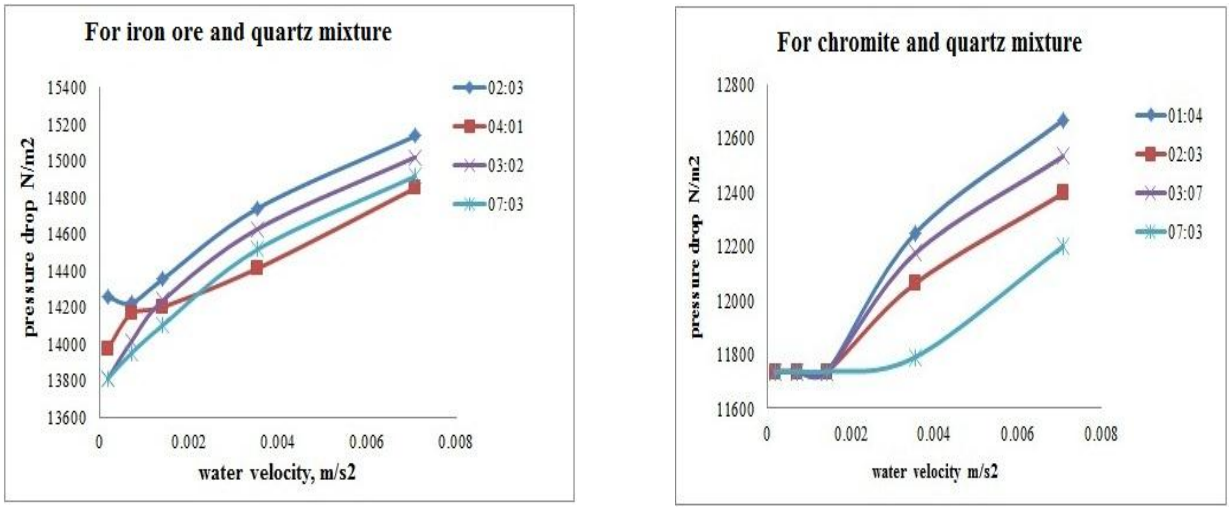

Fig.5.19 Variation of bed pressure drop with superficial water velocity for different weight ratio of mixtures results obtain from CFD simulation

Fig.5.19 represents the pressure drop increases as a function of superficial water velocity. When velocity increase the bed of the particles start to fluidized and pressure difference also increases. Hence the pressure drop increases with increase in superficial velocity. This nature occurs due to frictional resistance at particle surface and sudden expansion and contraction of the particles. This figure somehow agree with the experimental results i.e. pressure drop increases with increase in fluidized velocity.

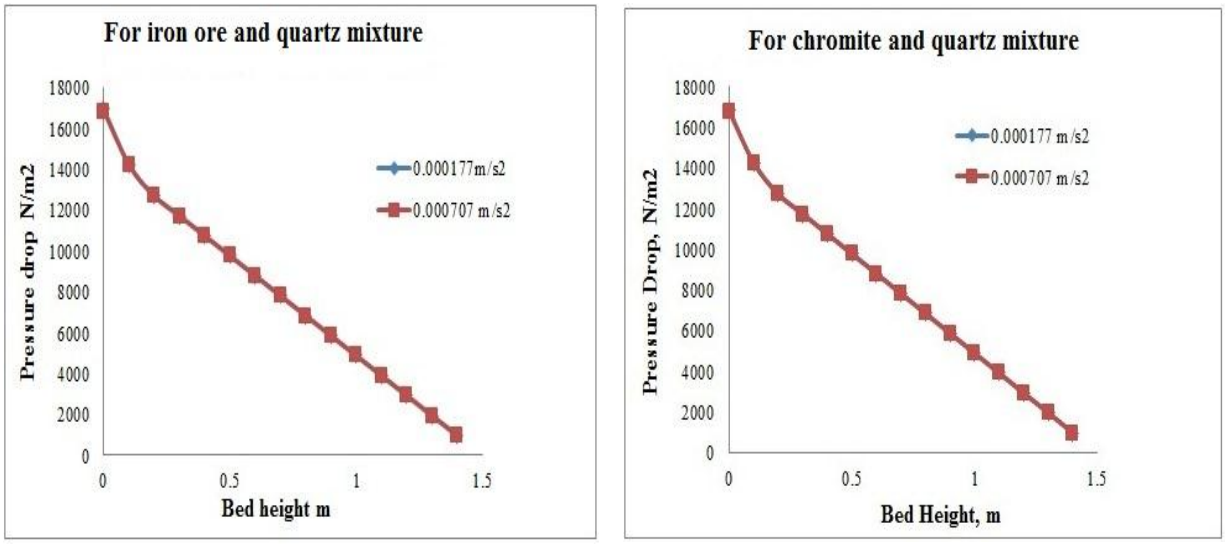

Fig.5.20 variation of pressure drop vs. bed height for different weight ratio of 40:60 for different velocity of mixtures results obtain from CFD simulation

Fig.5.20 shows that the pressure drop is a function of bed height. From the figure it is shows that the pressure drop gradually decreases with increase in bed height for two different bed heights for similar ratio of the mixture. This is due to when the bed height increases the upper portion of the column the bed voidage decreases and lower pressure drop is needed to fluidize a bed of mixture.

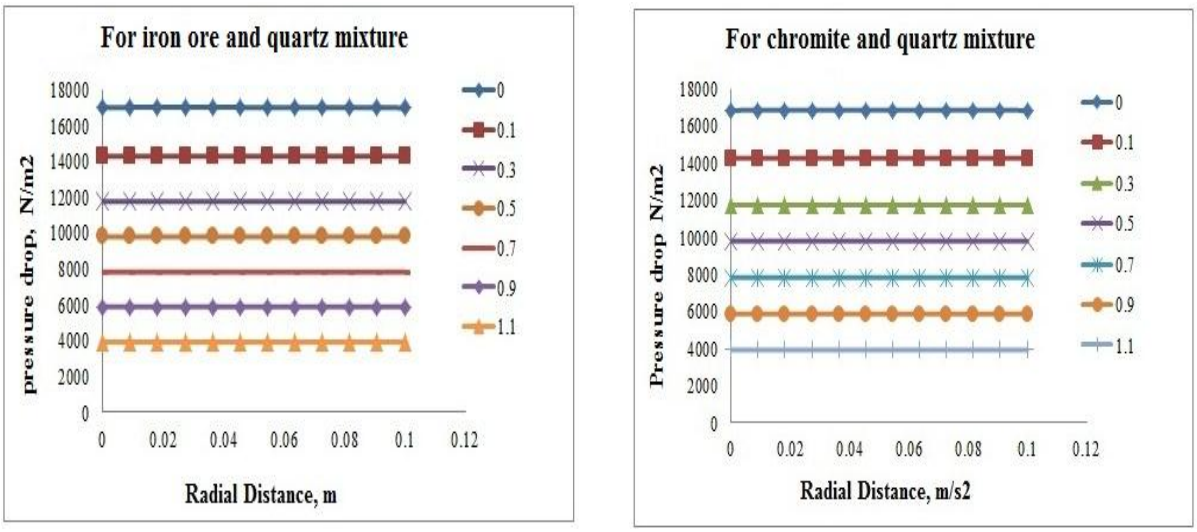

Fig.5.21 variation of pressure drop vs. radial distance for different bed height of mixtures results obtain from CFD simulation

Fig.5.21 represents the pressure drop also a function of radial position of the bed. When the radial distance of the bed increases the pressure drop gradually decreases. This figure shows that the different radial distance of the bed for iron ore and quartz mixture also the chromite and quartz mixture. In both cases results obtained from simulation is similar like pressure drop decreases with radial distance.

5.10 CONCLUSIONS

In this chapter, CFD simulation of hydrodynamics of liquid–solid fluidized bed has been carried out for different operating conditions by employing the Eulerian-Eulerian granular multiphase approach. The CFD simulation results have shown good agreement with experimental data for solid phase hydrodynamics in term of expanded bed height of the present experimental findings and liquid phase hydrodynamics in terms of phase velocities. The bed expansion values indicate that the drag model used in CFD simulation has satisfactorily described the solid-solid-liquid

phase phenomena. The bed expansion behaviour with variation in liquid velocity obtained from CFD simulation to some extent has corroborated the experimental findings. The good agreement between the values obtained from CFD simulation and experimental ones for the range of the present operating variables justify that the Eulerian-Eulerian multi-phase granular flow approach is capable to predict the overall performance of liquid–solid fluidized bed.

CHAPTER-6

CONCLUSION AND FUTURE SCOPE OF THE WORK

CHAPTER-6

CONCLUSION AND FUTURE SCOPE OF THE WORK

6.1 CONCLUSION

From the experimental result it is observed that the bed expansion for the mixture increases with increase in the weight fraction of flotsam in the mixture. For any given fluidizing medium, a mixing/segregation regime map can be drawn in terms of size ratio and density ratio of the particles. The bed expansion ratio is increases with increase in weight ratio flotsam. Liquid-solid system is the one process for segregation of particles having different in their density. It has been observed that bed expansion can be used as an important indicator for the misplacement of particles in a column and the component density ratio of the mixture is a variable that affects the segregation pattern of binary bed.

CFD simulation of hydrodynamics of liquid–solid fluidized bed has been carried out for different operating conditions by employing the Eulerian-Eulerian granular multiphase approach. The CFD simulation results have shown good agreement with experimental data for solid phase hydrodynamics in term of expanded bed height of the present experimental findings and liquid phase hydrodynamics in terms of phase velocities. The bed expansion values indicate that the drag model used in CFD simulation has satisfactorily described the solid-solid-liquid phase phenomena. The bed expansion behaviour with variation in liquid velocity obtained from CFD simulation to some extent has corroborated the experimental findings. Experimental result has shown an increase in bed expansion with liquid velocity, on the other hand CFD simulation has also shown slight increase in bed expansion. The CFD simulation exhibited a solid circulation pattern for all the operating conditions, which is consistent with the observations reported by various earlier investigators. The good agreement between the values obtained from CFD simulation and experimental ones for the range of the present operating variables justify that the Eulerian-Eulerian multi-phase granular flow approach is capable to predict the overall performance of liquid–solid fluidized bed.

6.2 FUTURE SCOPE OF THE WORK

In the present work, experiment can be carried out by using different size, density of material. This method here applied for small scale unit but it can be applied for large scale also i.e., industries for design and optimize the units. Modeling and simulation of binary solid-liquid system can be developing 3D techniques also by taking different size and density of materials.

REFERENCE

1. R. Escudiéa, N. Epsteina, J.R. Gracea, H.T. Bi. Effect of particle shape on liquid-fluidized beds of binary (and ternary) solids mixtures: segregation vs. mixing, Journal of Chemical Engineering Science 61 (2006) 1528 – 1539.

2. K.C. Biswal, T. Bhowmik, G.K. Roy, Prediction of minimum fluidization velocity for gas-solid fluidization of regular particles in conical vessels, Chem. Eng. J. 30 (1985) 57–62.

3. Maureen A. Howley, Benjamin J. Glasser. Hydrodynamics of a uniform liquid-fluidized bed containing a binary mixture of particles, Chemical Engineering Science 57 (2002) 4209 – 4226.

4. Trambouze, P., Euzen, J., 2004. Chemical Reactor, from Design to Operation. Technip, Paeis.

5. F. Depypere, J.G. Pieters, K. Dewettinck, Expanded bed height determination in a tapered fluidised bed reactor, Journal of Food Engineering 67 (2005) 353–359

6. N. Epstein, B.B. Pruden, Liquid fluidization of binary particle mixtures—III Stratification by size and related topics, Chemical Engineering Science 54 (1999) 401—415.

7. Jena, H.M., 2009. Hydrodynamic of Gas-Liquid-Solid Fluidized and Semi-Fluidized Beds, PhD thesis. National Institute of Technology, Rourkela

8. Rupesh K. Reddy, Jyeshtharaj B. Joshi, CFD modeling of solid–liquid fluidized beds of mono and binary particle mixtures, Chemical Engineering Science 64 (2009) 3641 – 3658.

9. S. Barghi, C.L. Briens, M.A. Bergougnou, Mixing and segregation of binary mixtures of particles in Liquid–solid fluidized beds, Powder Technology 131 (2003) 223– 233.

10. A. K. A. Juma and J. F. Richardson, Segregation and Mixing in Liquid Fluidized Beds, Chemical Engineering Science, vol. 38,No.6,pp.955-967,1983.

11.Renzo Di Felice, Hydrodynamics of liquid solid fluidization, Chemical Engineering Science, Vol. 50, No, 8, pp. 1213-1245,1995.

12. B. Formisani and R. Girimonte, Experimental Analysis of the Fluidization Process of Binary Mixtures of Solid, Dipartimento di Ingegneria Chimica e die Materiali, Università della Calabria

13. M.G. Rasul, V. Rudolph, F.Y. Wang, Particles separation using fluidization techniques, Int. J. Miner. Process. 60 2000 163–179

14. R. Escudiéa, N. Epsteina, J.R. Gracea, H.T. Bi. Effect of particle shape on liquid-fluidized beds of binary (and ternary) solids mixtures: segregation vs. mixing, Journal of Chemical Engineering Science 61 (2006) 1528 – 1539

15. Maureen A. Howley, Benjamin J. Glasser, Hydrodynamics of a uniform liquid-fluidized bed containing a binary mixture of particles, Chemical Engineering Science 57 (2002) 4209 – 4226.

16. Sankarshana Talapuru, J S N Murthyy, S Nandanaz, Phani Kiran S V G R, V Rameshy, Hydrodynamic Characteristics of Liquid-Solid Fluidization of Binary Mixtures in Tapered Beds, 2010 ECI Conference on The 13th International Conference on Fluidization - New Paradigm in Fluidization Engineering.

17. S. Barghi, C.L. Briens, M.A. Bergougnou, Mixing and segregation of binary mixtures of particles in Liquid–solid fluidized beds, Powder Technology 131 (2003) 223– 233.

18. N. Epstein, B.B. Pruden, Liquid fluidization of binary particle mixtures—III Stratification by size and related topics, Chemical Engineering Science 54 (1999) 401—415.

19. A.K. Mukherjee, B.K. Mishra, Experimental and simulation studies on the role of fluid velocity during particle separation in a liquid–solid fluidized bed, Int. J. Miner. Process. 82 (2007) 211–221

20. M.G. Rasul, V. Rudolph, M. Carsky, Segregation in binary and ternary liquid fluidized beds, Powder Technology 126 (2002) 116– 128

21. Fan, L.S., Muroyama, K., Chern, S.H., 1982. Hydrodynamic characteristics of inverse fluidization in liquid–solid and gas–liquid–solid systems. The Chemical Engineering Journal 24, 143-150.

22. Bruno Formisani, Rossella Girimontey, Tiziana Longoz, The Fluidization Pattern of Density-Segregating Two-Solid Beds, 2007 ECI Conference on The 12th International Conference on Fluidization - New Horizons in Fluidization Engineering

23. Y.Peng, L.T.Fan, Hydrodynamic characteristics of fluidization in liquid-solid tapered beds, Chemical Engineering Science 52 (14) (1997) 2277 – 2290

24. K. Ganesh Palappan, P.S.T. Sai, Studies on segregation of binary mixture of solidsin a continuous fast fluidized bed Part I. Effect of particle density, Chemical Engineering Journal 138 (2008) 358–366

25. A. R. Khan and J. F. Richardson, Pressure Gradient and Friction Factor for Sedimentation and Fluidization of Uniform Spheres in Liquids, Chemical Engineering Science. Vol. 45, No. 1, pp. 255-265, 1990

26. Paola Lettieri , Renzo Di Felice , Roberta Pacciani , Olumuyiwa Owoyemi, CFD modeling of liquid fluidized beds in slugging mode, www.elsevier.com/locate/powtec, Powder Technology 167 (2006) 94–103

27. Rupesh K. Reddy, Jyeshtharaj B. Joshi, CFD modeling of solid–liquid fluidized beds of mono and binary particle mixtures, Chemical Engineering Science 64 (2009) 3641 – 3658.

28. R. Panneerselvam, S. Savithri, G.D. Surender, CFD based investigations on hydrodynamics and energy dissipation due to solid motion in liquid fluidised bed, Chemical Engineering Journal 132 (2007) 159–171

29. Luca Mazzei, PaolaLettieri, CFD simulations of expanding/contracting homogeneous fluidized beds and their transition to bubbling, Chemical Engineering Science 63 (2008) 5831-5847

30. Shuyan Wang, Xiaoqi Li, Yanbo Wu, Xin Li, Qun Dong, and Chenghai Yao, Simulation of Flow Behavior of Particles in a Liquid-Solid Fluidized Bed, Ind. Eng. Chem. Res. 2010, 49, 10116–10124

31. Long Fan, John Gracey, Norman Epsteinz, CFD Simulation of a Liquid-Fluidized Bed of Binary Particles, 2010 ECI Conference on the 13th International Conference on Fluidization - New Paradigm in Fluidization Engineering

32. Jack T. Cornelissena, Fariborz Taghipoura, Renaud Escudiea, Naoko Ellisa, John R. Grace, CFD modelling of a liquid–solid fluidized bed, Chemical Engineering Science 62 (2007) 6334 – 6348

33. Olumuyiwa Owoyemi, Paola Lettieri, A CFD Study into the Influence of the Particle-Particle Drag Force on the Dynamics of Binary Gas Solid Fluidized Beds, Department of Chemical Engineering, University College London, Torrington Place, London, WC1E 7JE, UK.

34. Olumuyiwa Owoyemi, Luca Mazzei, and Paola Lettieri, CFD Modeling of Binary-Fluidized Suspensions and Investigation of Role of Particle–Particle Drag on Mixing and Segregation, AIChE J, 53: 1924–1940, 2007

35. Fariborz Taghipour, Naoko Ellis, Clayton Wong, Experimental and computational study of gas–solid fluidized bed hydrodynamics, Chemical Engineering Science 60 (2005) 6857 – 6867

36. G.R. Kumar Reddy And J.B. Joshi, CFD Simulation of Fluid-Particle and Particle-Particle Interaction in Packed and Fluidized Beds, Institute of Chemical Technology, Matunga, Mumbai-400 019, INDIA

37. Matteo Chiesaa, Vidar Mathiesenb, Jens A. Melheimc, Britt Halvorsend, Numerical simulation of particulate flow by the Eulerian–Lagrangian and the Eulerian–Eulerian approach with application to a fluidized bed, Computers and Chemical Engineering 29 (2005) 291–304

38. Scott Cooper, Charles J. Coronella T, CFD simulations of particle mixing in a binary fluidized bed, Powder Technology 151 (2005) 27– 36

39. Joshi J. B., Vitankar, V. S., Dhotre, M. T., 2002. A low Reynolds number k–e model for the prediction of flow pattern and pressure drop in bubble column reactors. Chemical Engineering Science 57, 3235 – 3250

40. Mitra-Majumdar, D., Farouk, B., Shah, Y. T., 1997. Hydrodynamic modeling of three- phase flows through a vertical column. The Chemical Engineering Science 52, 4485–4497

41. Li, Y., Zhang, J., Fan, L. S., 1999. Numerical simulation of gas–liquid–solid fluidization systems using a combined CFD–VOF–DPM method, bubble wake behavior. Chemical Engineering Science 54, 5101–5107

42. Andre Bakker, Introduction to CFD, Applied Computational Fluid Dynamics, www.bakker.org

43. Wen Y. Soung, Bed Expansion in Three-phase Fluidization, Ind. Eng. Chem. Process Des. Dev., Vol. 17, No. 1, 1978 33

44. H.M. Jenaa, B.K. Sahoo, G.K. Roya, B.C. Meikap, Characterization of hydrodynamic properties of a gas–liquid–solid three-phase fluidized bed with regular shape spherical glass bead particles, Chemical Engineering Journal (2008)

45. Haibo Yu and Bruce E. Rittmann, Predicting Bed Expansion and Phase Holdups for Three-Phase Fluidized-Bed Reactors with and Without Biofilm, Wat. Res. Vol. 31, No. 10. pp. 2604-2616, 1997

46. X Hu, The segregation in the binary-solid liquid fludized bed, Chemical Engineering Technology, 25 (2002) 9

47. R. Panneerselvam, S.Savithri, G.D.Surender, CFD simulation of hydrodynamics of gas–liquid–solid fluidised bed reactor, Chemical Engineering Science 64 (2009) 1119-1135

48. Huilin Lu, ShuyanWang,Yunhua Zhao, LiuYang, Dimitri Gidaspow, Jiamin Ding, Prediction of particle motion in a two-dimensional bubbling fluidized bed using discrete hard-sphere model, Chemical Engineering Science 60 (2005) 3217 – 3231